7

Magnetic domain walls

MAGNETIC DOMAIN WALLS MAGNETIC HYSTERESIS

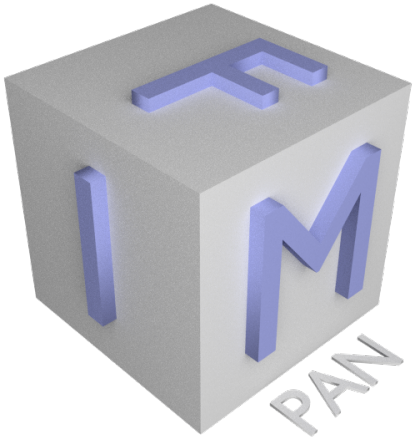

Poznań 2019

Maciej Urbaniak

7

Magnetic domain walls

- Domain walls in bulk materials cont.
- Domain walls in thin films
- Domain walls in 1D systems
- Domain wall motion

Bloch versus Néel wall

- From previous lectures we know **Bloch** and Néel domain walls.

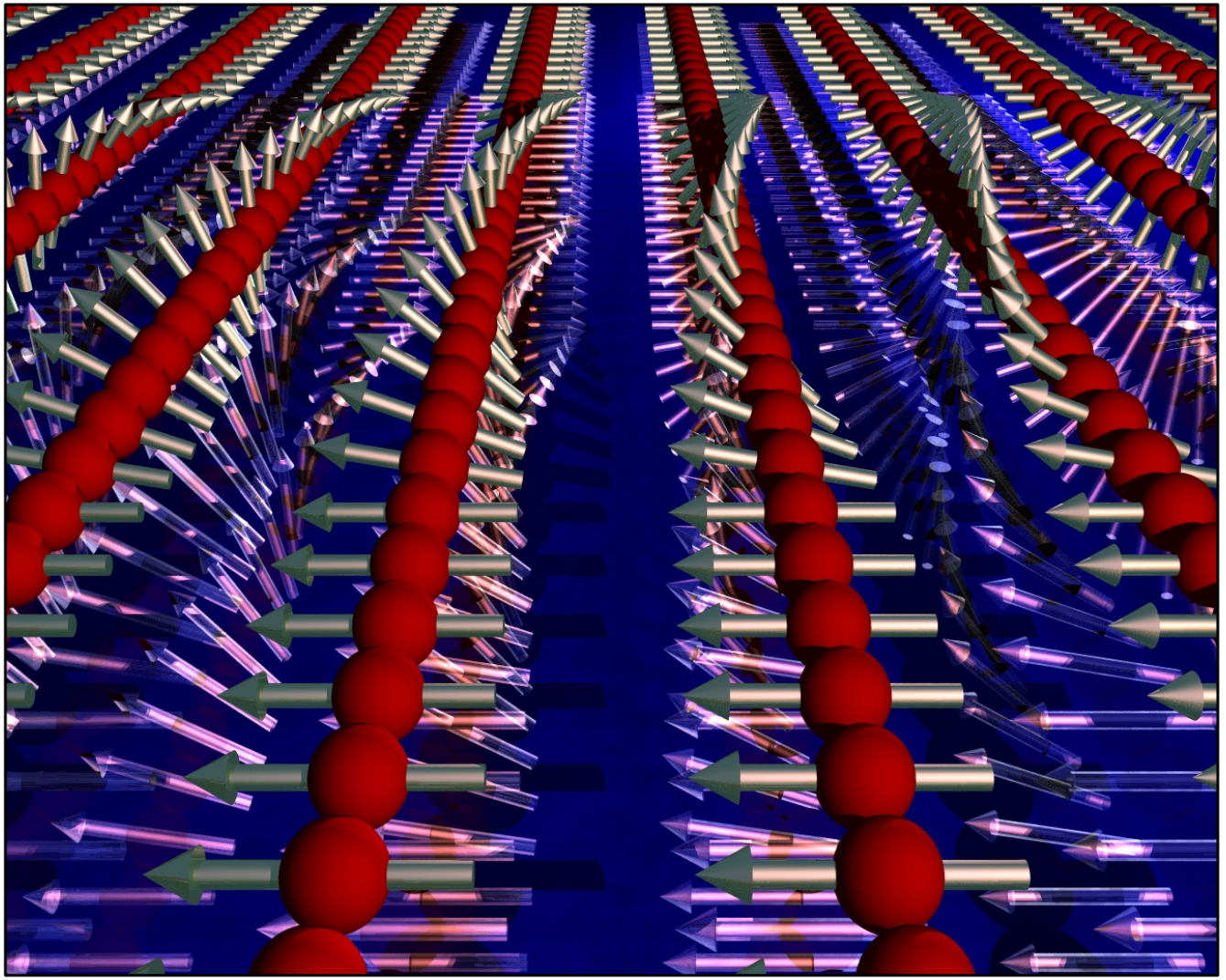

- Schematic view of the magnetic moments orientation of the Bloch wall in easy plane anisotropy sample
- The magnetic moments rotate gradually about the axis perpendicular to the wall

Bloch wall – right or left handedness

Chirality – the object cannot be mapped to its mirror image by rotations and translations alone

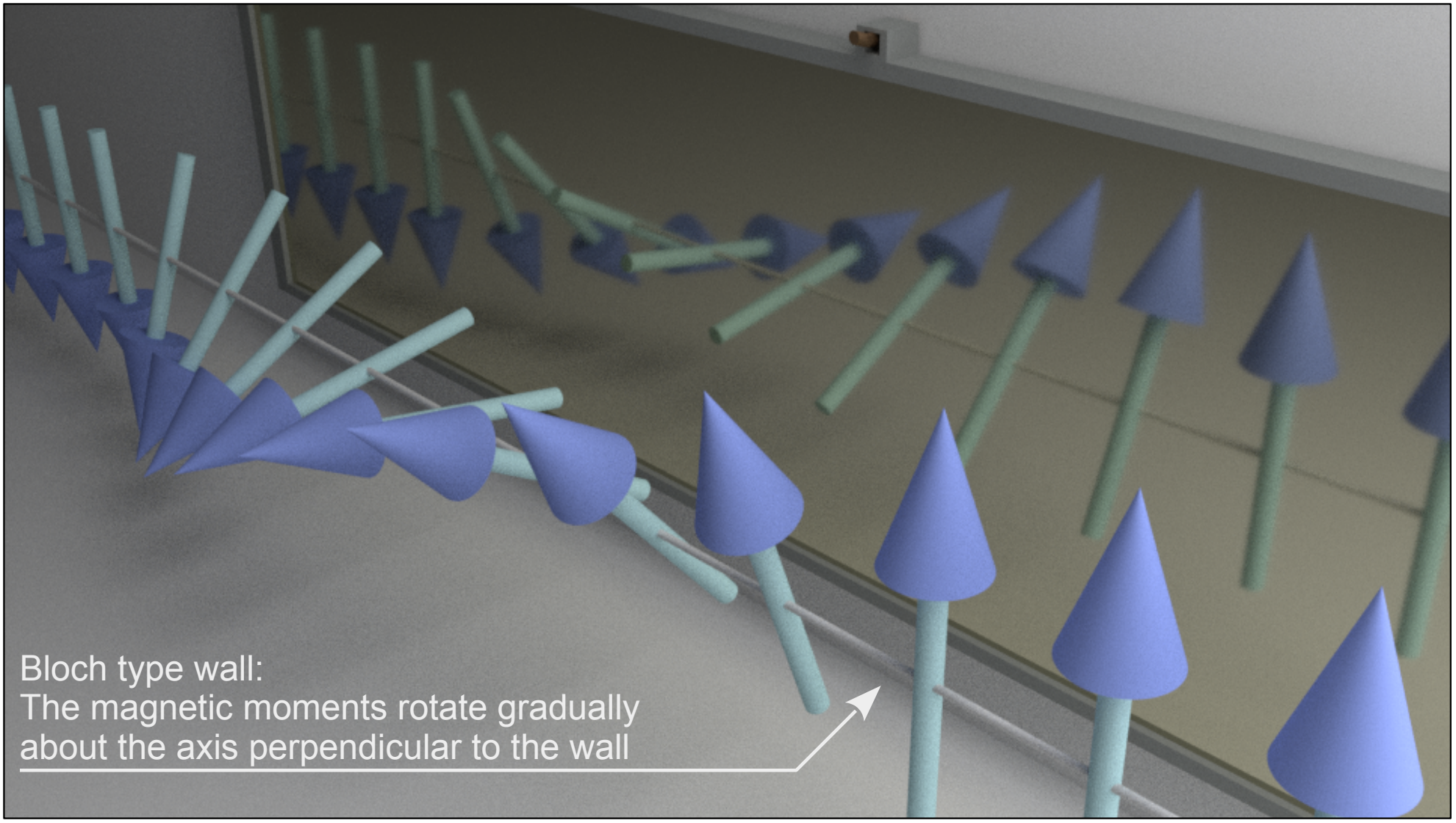

Néel walls come in two handednesses too.

Bloch versus Néel wall

- From previous lectures we know **Bloch** and Néel domain walls.

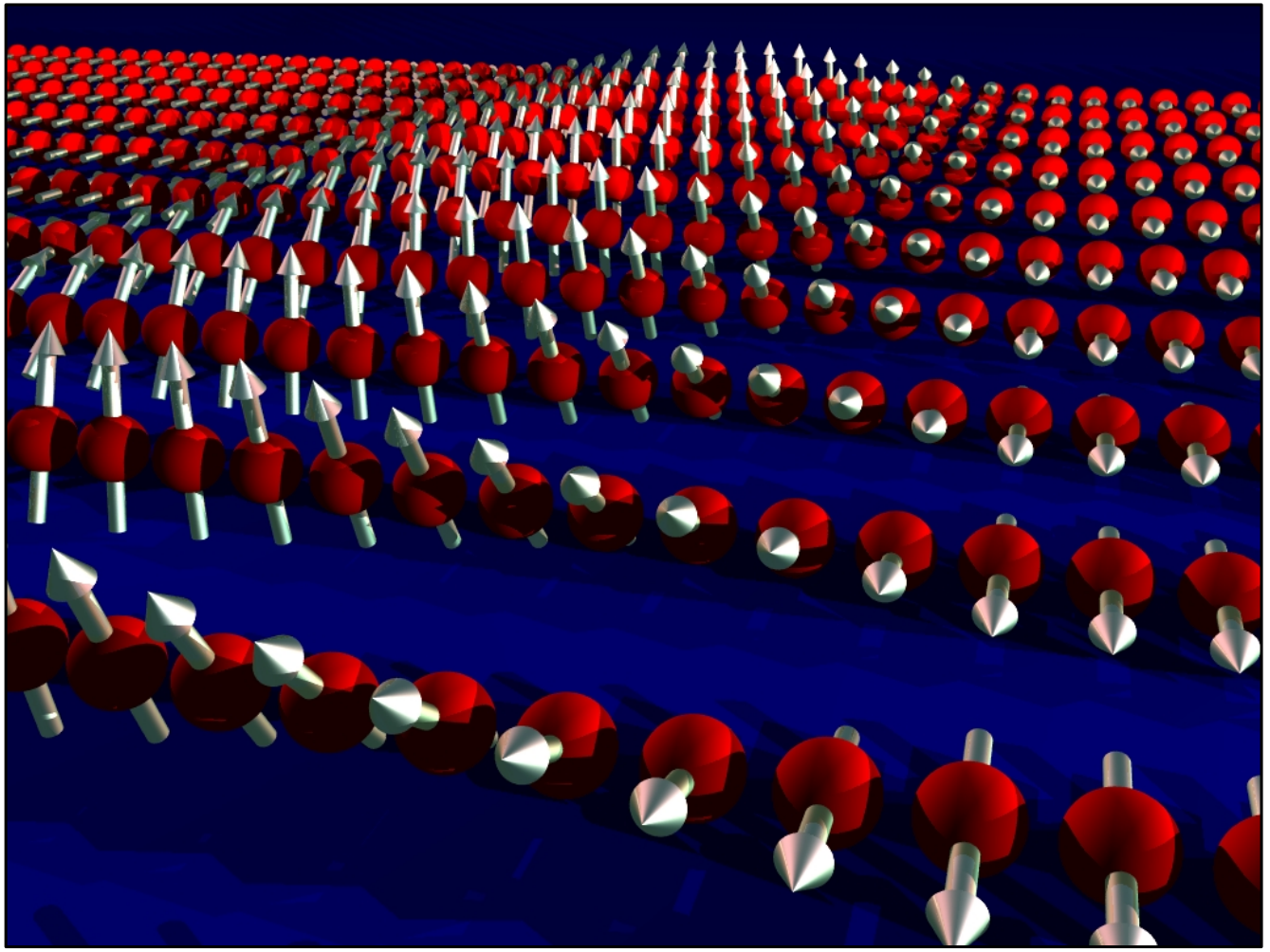

- To note is that when the Bloch wall in easy plane anisotropy sample crosses the surface of the sample the magnetic moments within the wall are **not parallel** to the surface
- **Magnetic charges** appear on the surface

Bloch versus Néel wall

- From previous lectures we know **Bloch** and Néel domain walls.

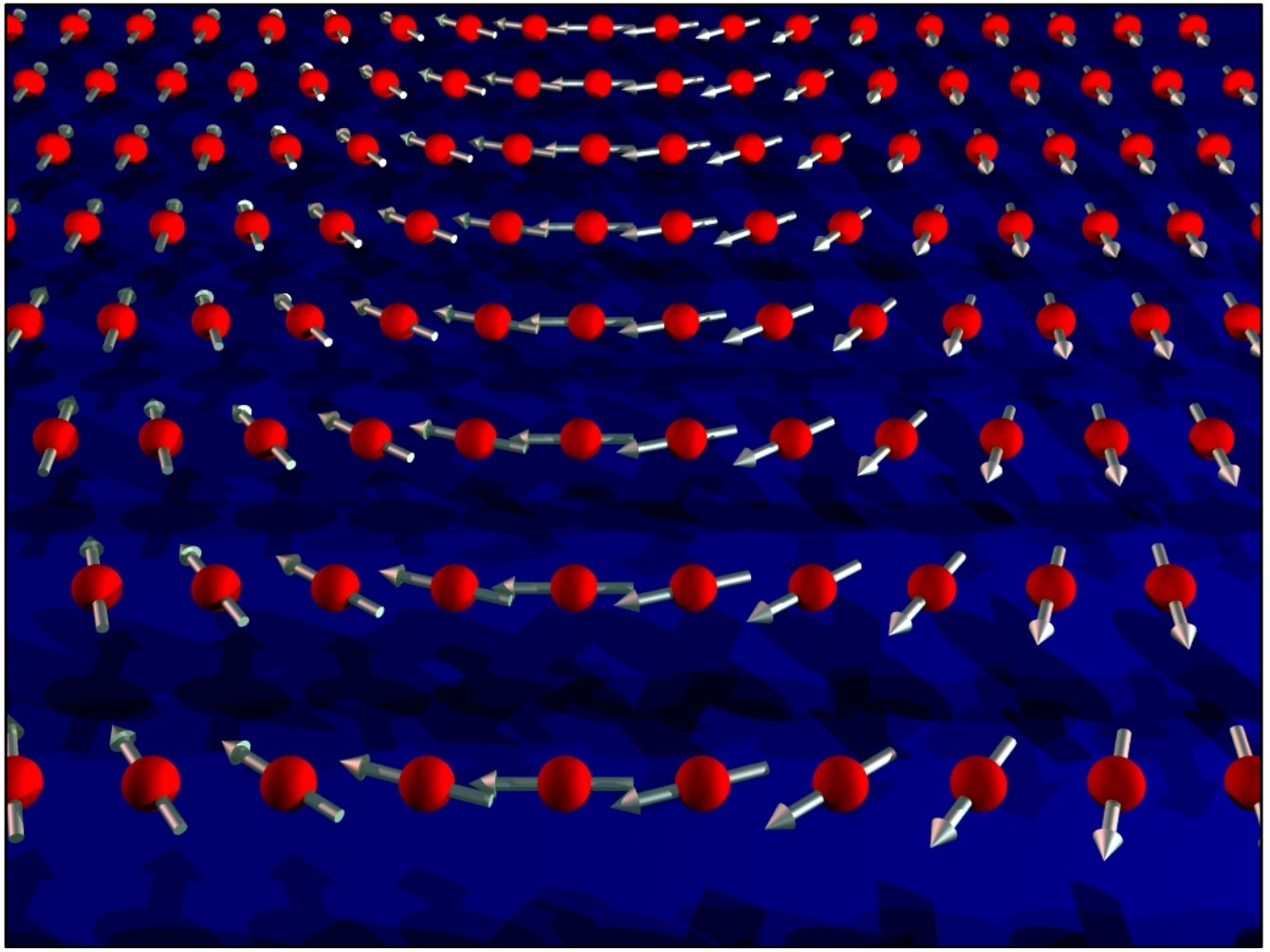

- Schematic view of the Néel wall
- Magnetic moments within Néel wall rotate along direction parallel to the wall
- To note is that when the Néel wall in easy plane anisotropy sample crosses the surface of the sample the magnetic moments within the wall are **parallel** to the surface

Bloch versus Néel wall

- The rotation of magnetic moments within the Néel wall creates volume magnetic charges.
- Assuming the following orientation of magnetization within Néel wall*:

$$\theta_{x\ axis}=\arctan(x);\qquad M_x=\cos(\theta_{x\ axis})\qquad M_y=\sin(\theta_{x\ axis})\qquad M_z=0$$

we obtain for the volume charge of the wall:

$$\rho_{magn}=-\nabla\cdot\vec{M}=-\left(\frac{\partial}{\partial x}M_x+\frac{\partial}{\partial y}M_y\right)=\frac{x}{(1+x^2)^{3/2}}$$

- Néel wall creates volume magnetic charges of opposite signs
- Néel wall, contrary to Bloch wall, is a source of magnetic field in an infinite crystal
- Néel wall corresponds to a line of magnetic dipoles

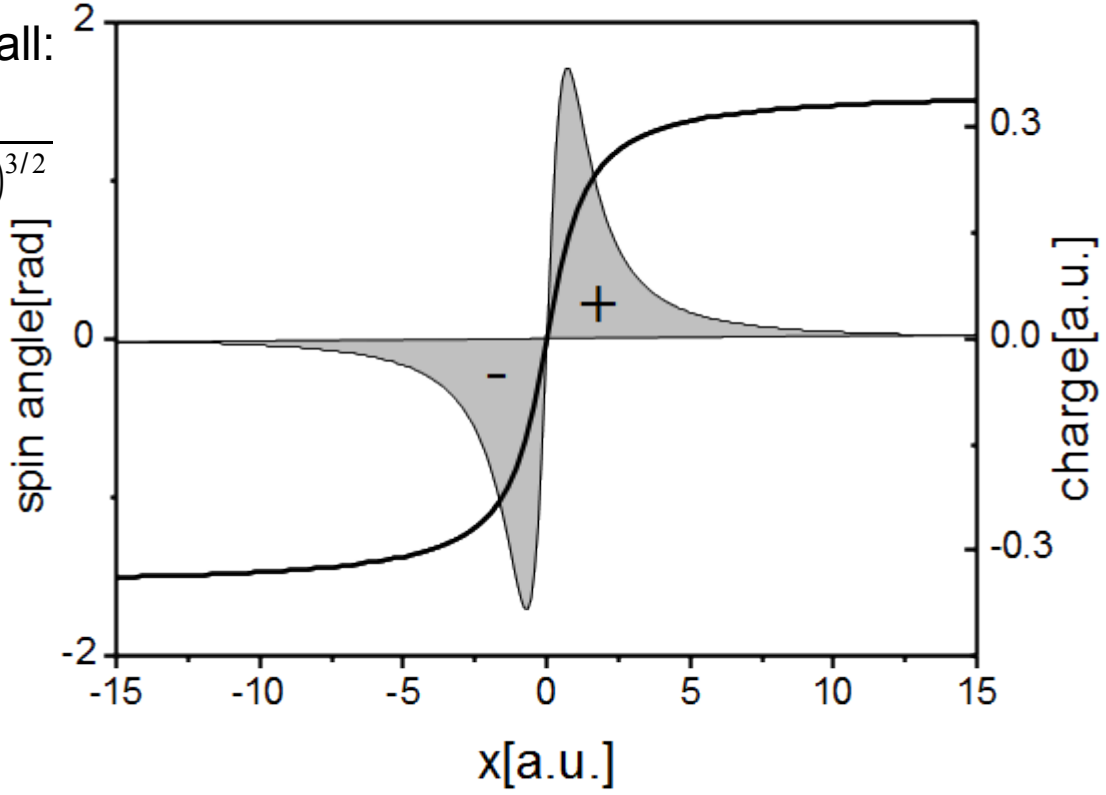

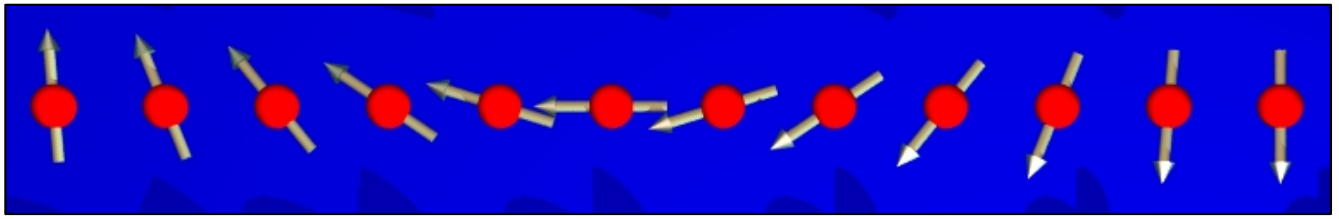

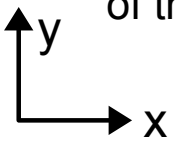

*this is just an approximation of the actual wall profile

Bloch wall in material with higher order anisotropy

- In uniaxial anisotropy material the energy is given by:

$$E_u = K_1 \sin^2\phi + K_2 \sin^4\phi$$

- In the previous derivation of the Bloch wall profile we have neglected the second order anisotropy constant K_2. It can be shown [1] that the wall profile with $K_2 \neq 0$ is given by:

$$\tan\phi = \sqrt{1+\kappa}\,\sinh\left(\frac{x}{\sqrt{A/K_1}}\right)$$

$$\kappa = K_2/K_1$$

- Parameter κ must be larger than -1, otherwise the two domains are not stable [1]*.
- On approaching κ=-1 the wall divides into **two 90°**-walls which may, if the effective anisotropy is modified, split into two creating new domain.
- Widened walls are common in cubic anisotropy materials.

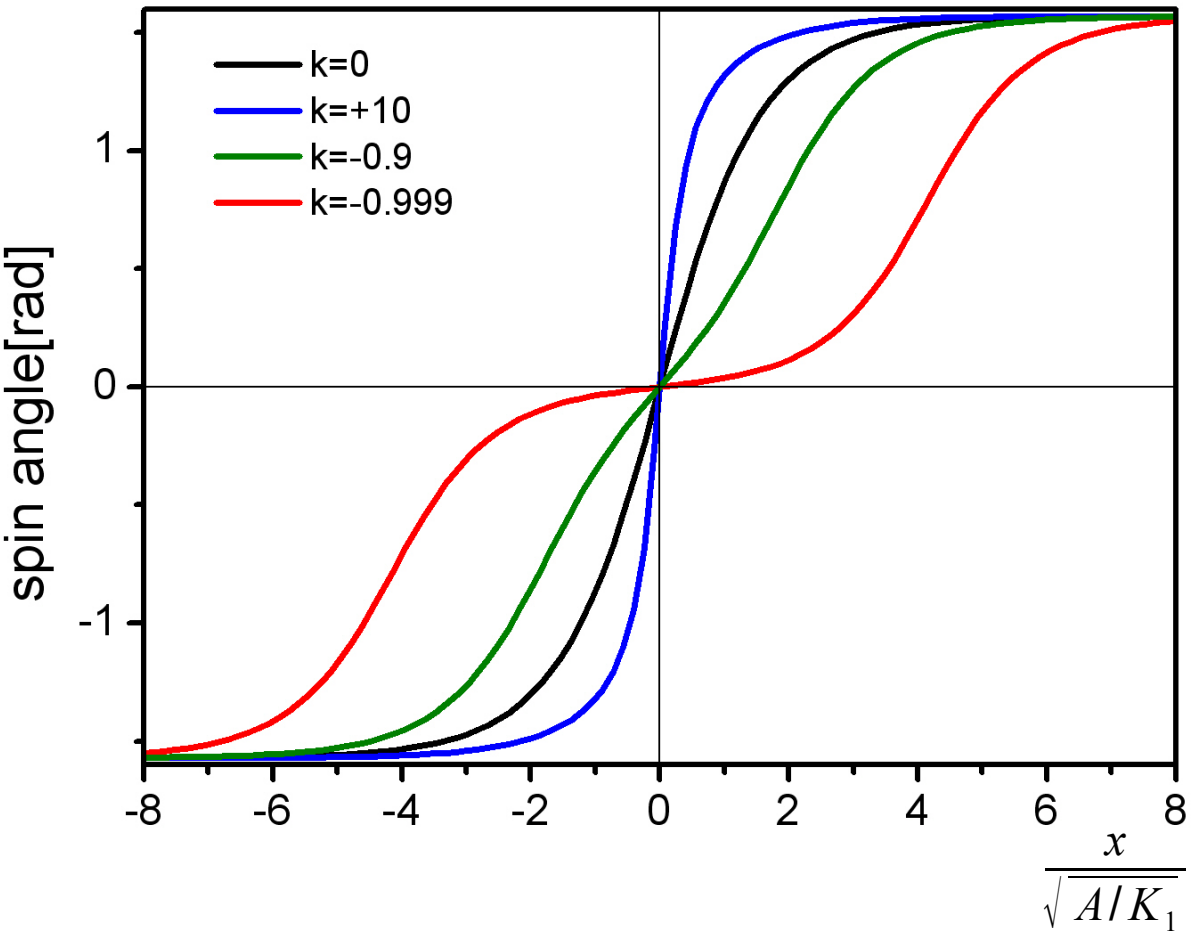

graphics based on Fig.3.60 from [1]: A. Hubert, R. Schäfer, Magnetic domains: the analysis of magnetic microstructures, Springer 1998

*the magnetization with spin angle 0 would have lower energy than for ±π/2

Bloch wall in material with higher order anisotropy

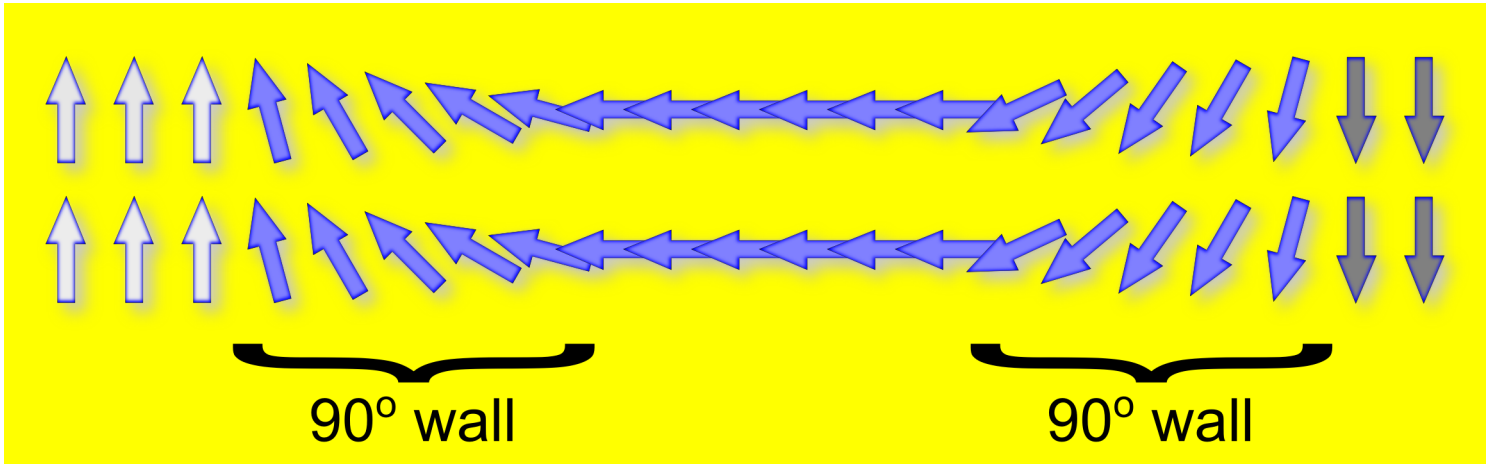

- Parameter κ must be larger than -1, otherwise the two domains are not stable [1]*.
- On approaching κ=-1 the wall divides into **two 90°**-walls which may, if the effective anisotropy is modified, split into two creating new domain.
- Widened walls are common in cubic anisotropy materials.

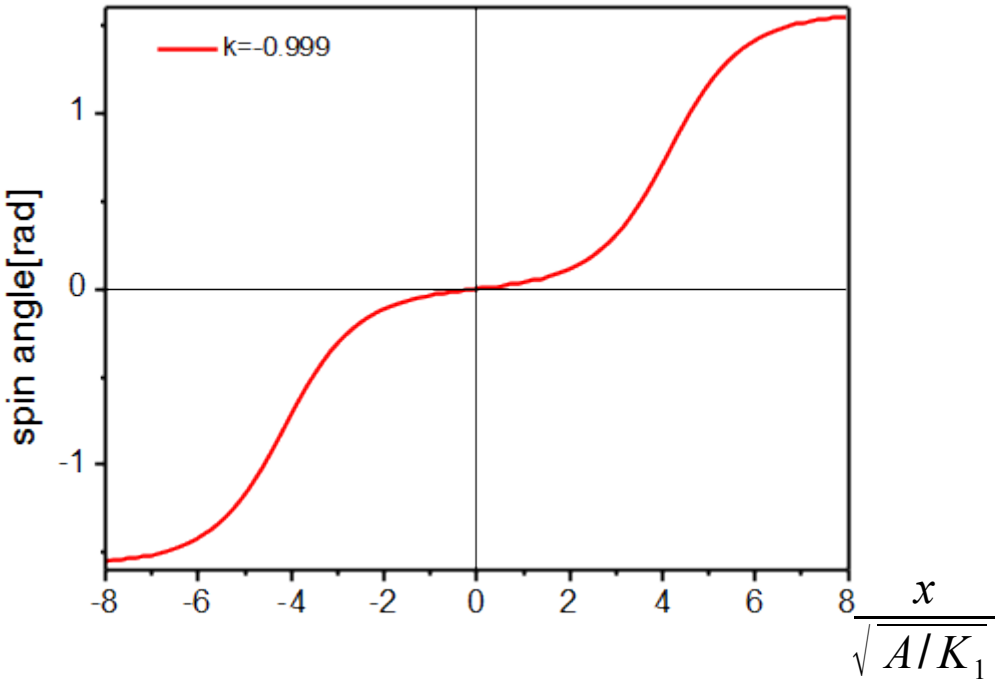

graphics based on Fig.3.60 from [1]: A. Hubert, R. Schäfer, Magnetic domains: the analysis of magnetic microstructures, Springer 1998

Bloch wall in material with higher order anisotropy

- Peculiarities of the wall profile influences the evaluation of wall width [1].
- For κ<-0.5 the wall profile has three points of inflection and the width is defined with the tangents in the outer inflection points (●).
- For other cases the thickness is defined as previously.

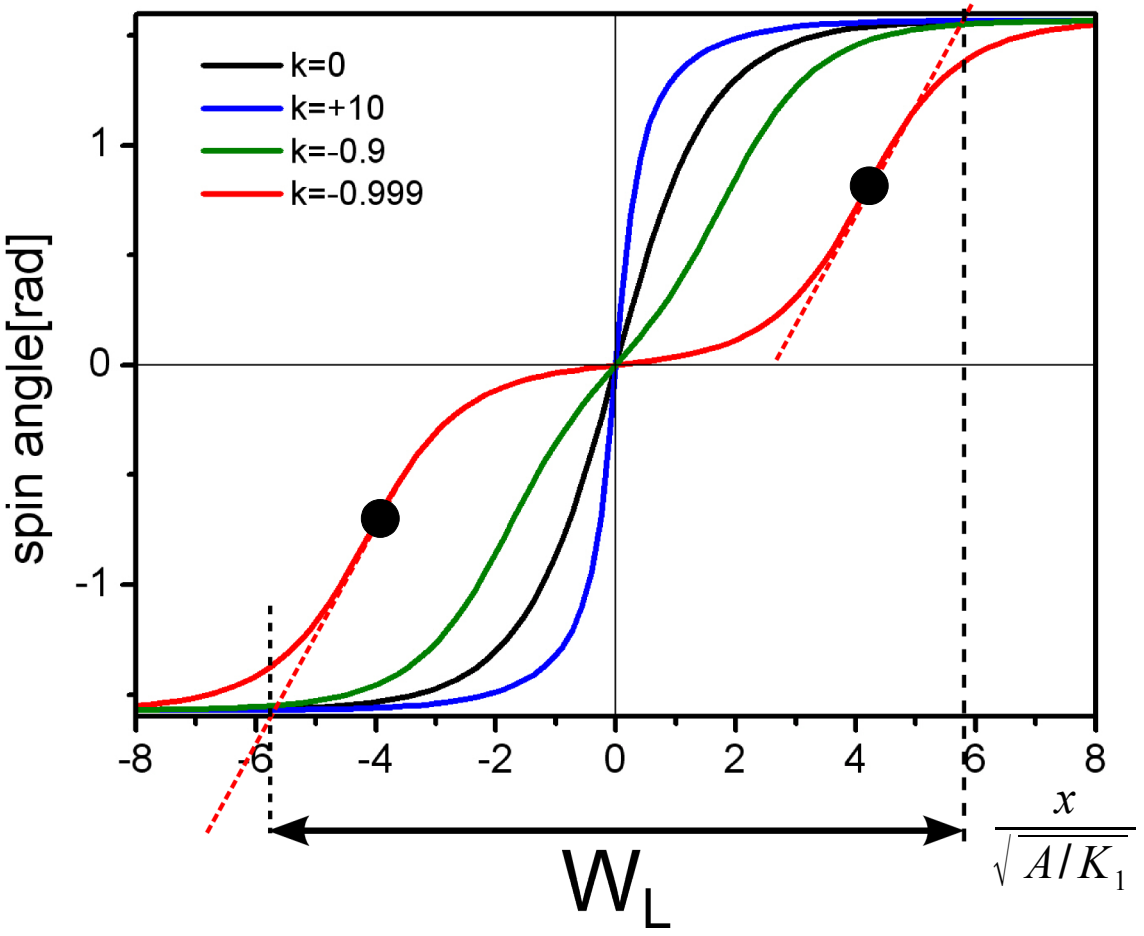

graphics based on Fig.3.60 from [1]: A. Hubert, R. Schäfer, Magnetic domains: the analysis of magnetic microstructures, Springer 1998

Domain walls in cubic anisotropy crystals

- In contrast to previously analyzed uniaxial anisotropy materials cubic anisotropy results in 3 or 4 easy axes (6 or 8 easy orientations of magnetization)
- In positive anisotropy crystals the preferred orientations are along <100> directions
- In negative anisotropy crystals the preferred orientations are along <111> directions

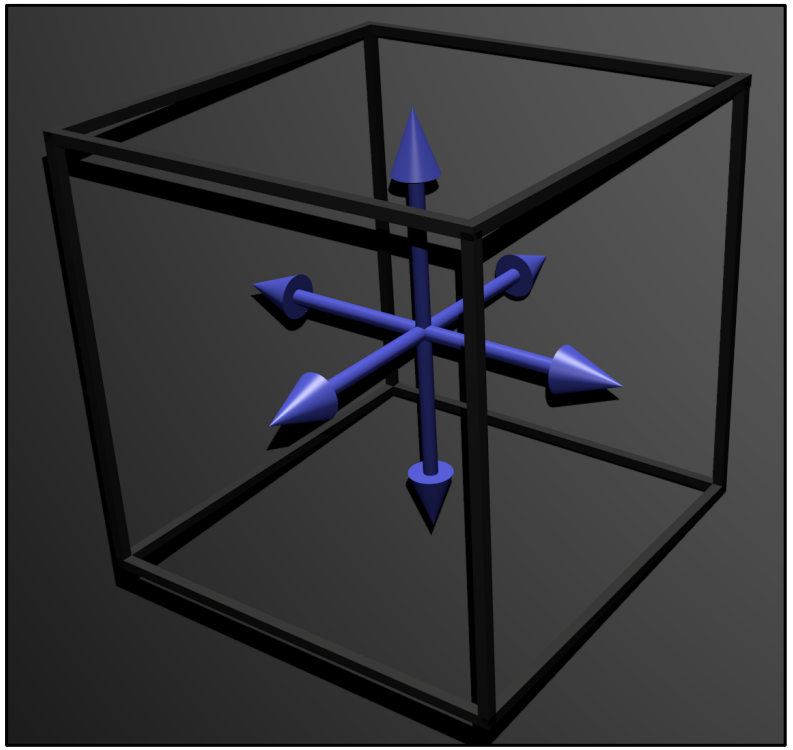

Preferred magnetization orientations
in Fe bulk crystals*
3 easy axes

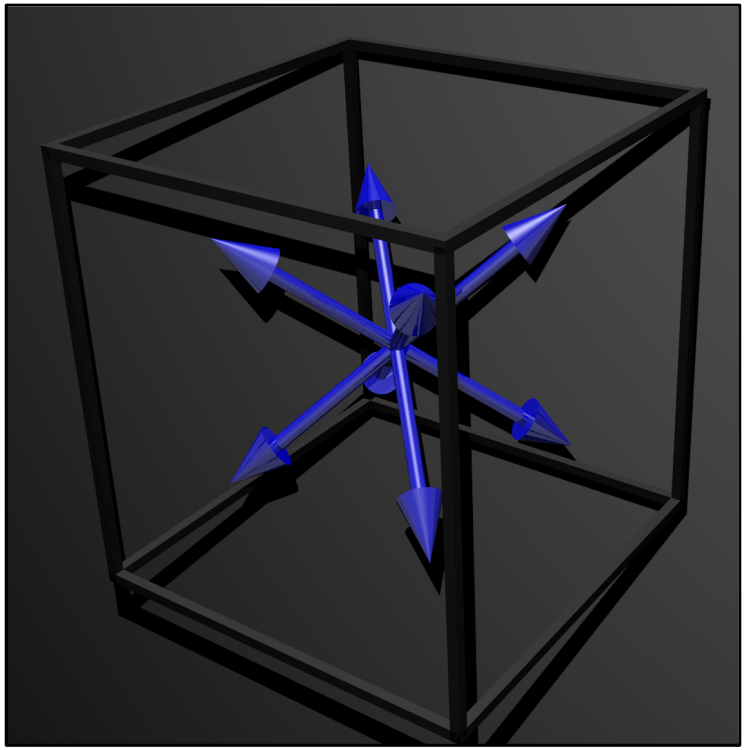

Preferred magnetization orientations
in Ni bulk crystals
4 easy axes

*without stress, external field etc.

Domain walls in cubic anisotropy crystals

- In positive anisotropy crystals the possible angles between unperturbed domain magnetizations are 90° and 180° (see the previous slide)
- In negative anisotropy crystals the allowable angles are 71° and 109°:

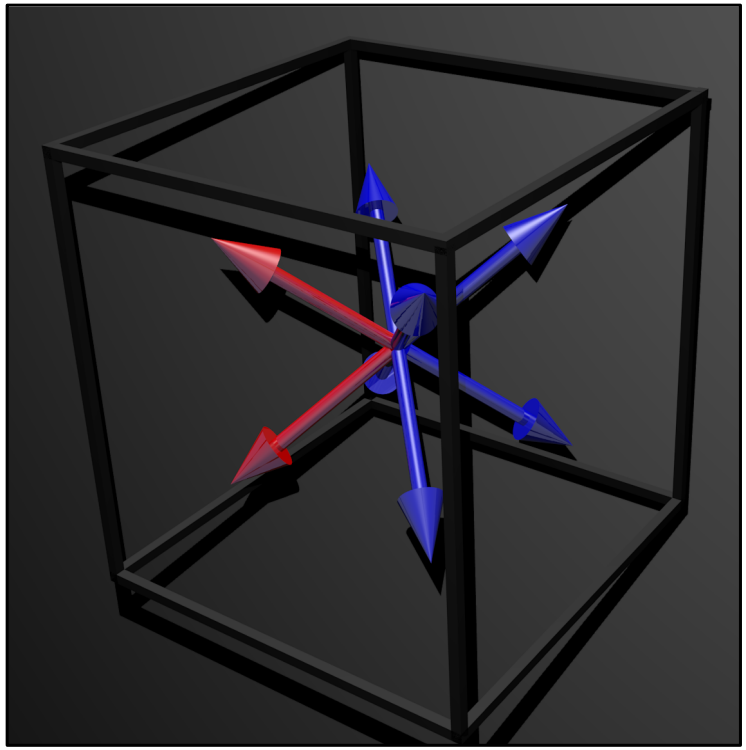

70.528°

109.472°

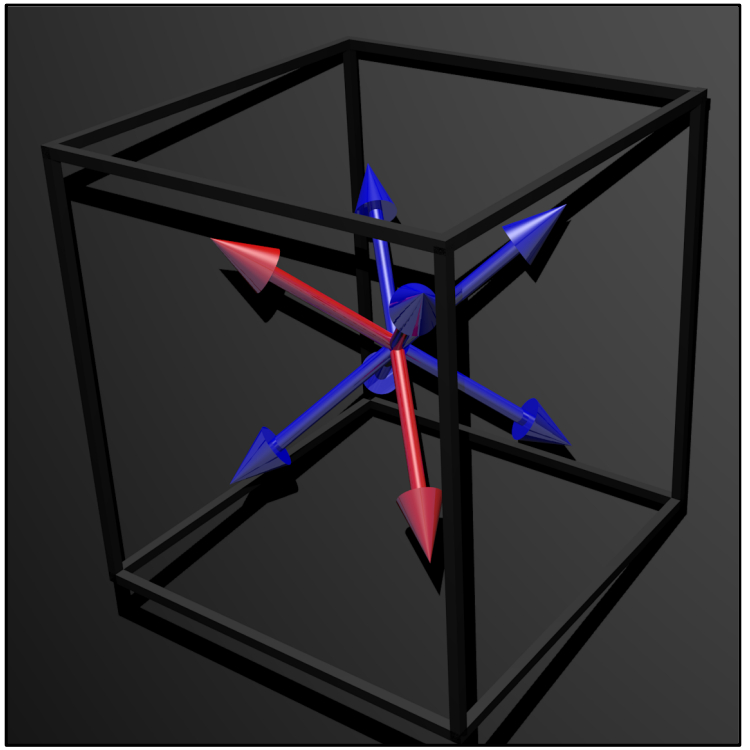

Preferred magnetization orientations in Ni bulk crystals
4 easy axes

*without stress, external field etc.

Domain walls in cubic anisotropy crystals

- Due to anisotropy the energy of the domain wall depends on its orientation relative to the crystal axes:

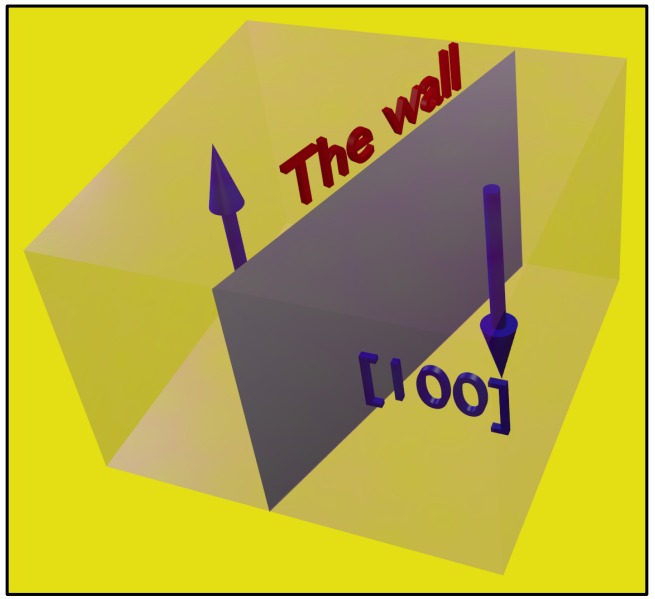

- Magnetostatic energy does not restrict the orientation of domain wall
- We assume the magnetization direction to rotate within the wall from [100] to its opposite direction
- In static equilibrium no field can exist in cubic material with 180° wall [1]:

-the field parallel to [100] direction would force the wall to move as in uniaxial crystals

-the field component within the (100) plane would favor other domains

The preferred orientation of 180° wall in (100) oriented transformer steel favors wall shapes as shown, in contrast to straight, perpendicular walls (image from A. Hubert [1] - Fig. 3.64)

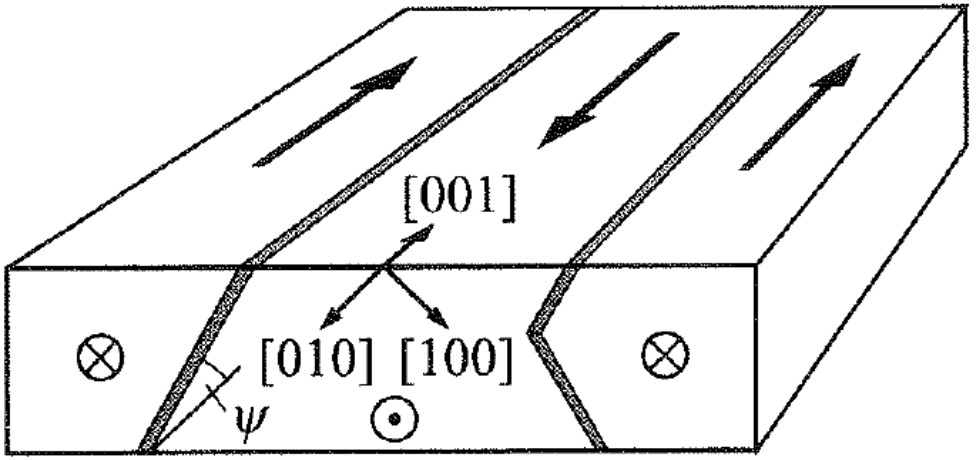

Domain walls in thin films

- Magnetic films are defined as **thin** if their thickness is comparable with Bloch wall width [1].

- A Bloch and Néel walls can be approximated by an infinite elliptical cylinder, of height equal to the thickness of the film [1,2], placed between regions of opposite magnetization:

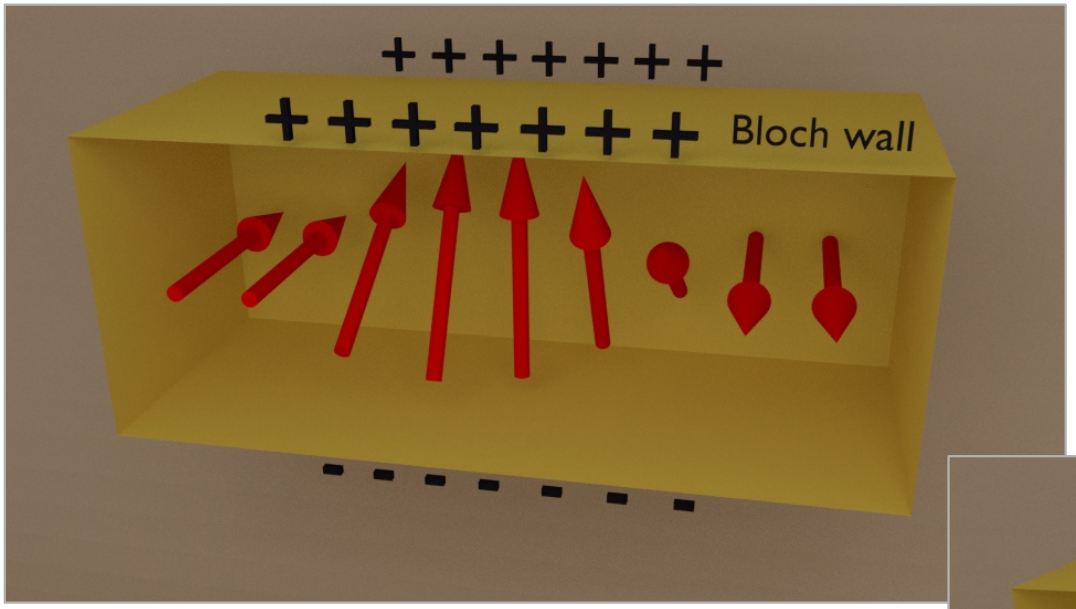

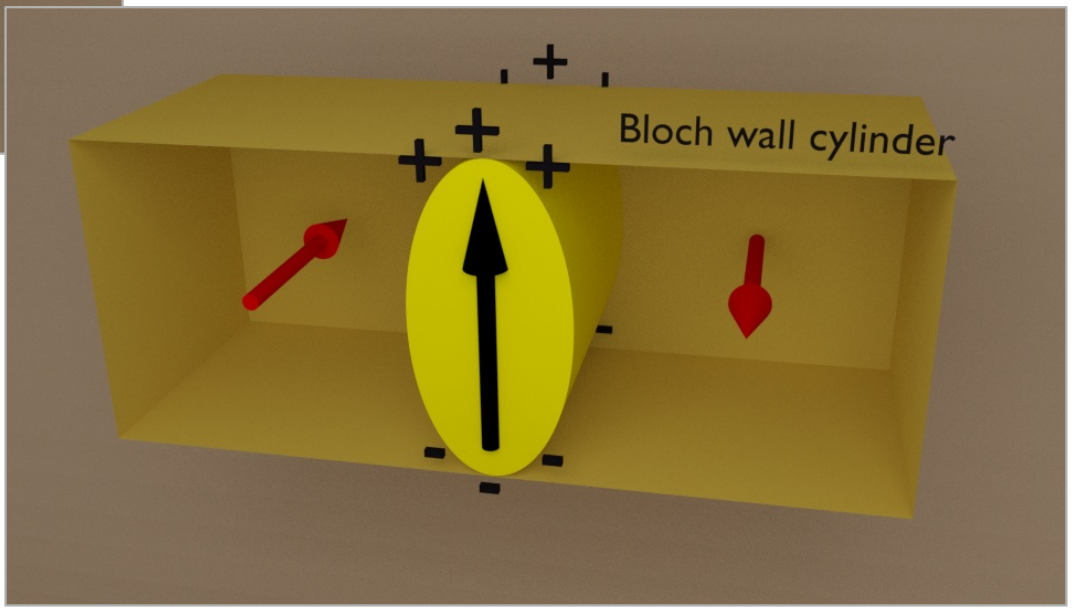

- Demagnetizing factors of the cylinders can be approximated with expressions for ellipsoids.

Domain walls in thin films

- Magnetic films are defined as **thin** if their thickness is comparable with Bloch wall width [1].

- A Bloch and Néel walls can be approximated by an infinite elliptical cylinder, of height equal to the thickness of the film [1,2], placed between regions of opposite magnetization:

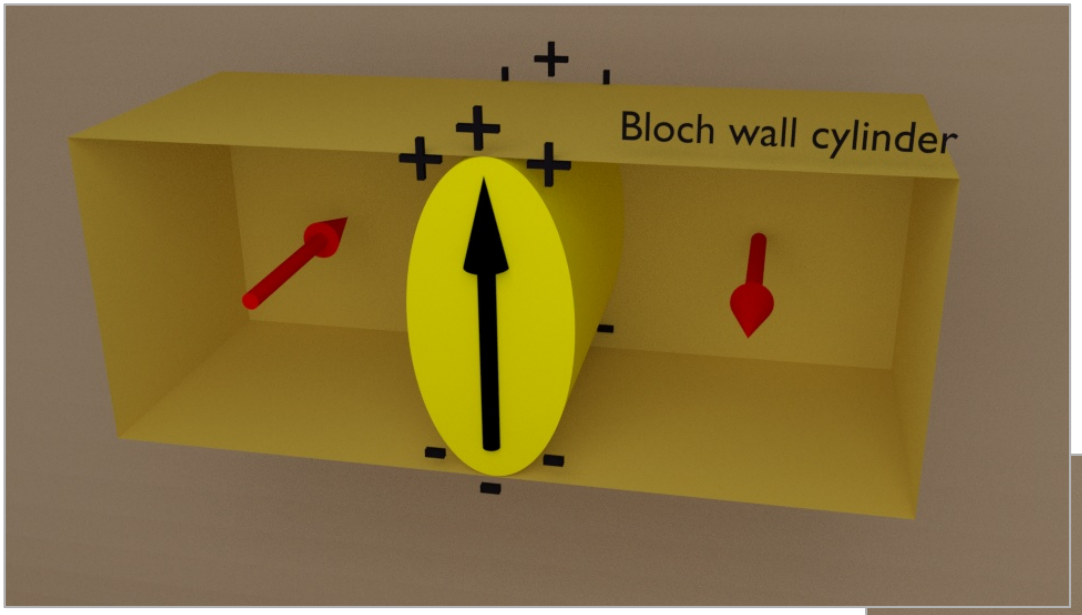

- Demagnetizing factors of the cylinders can be approximated with expressions for ellipsoids.

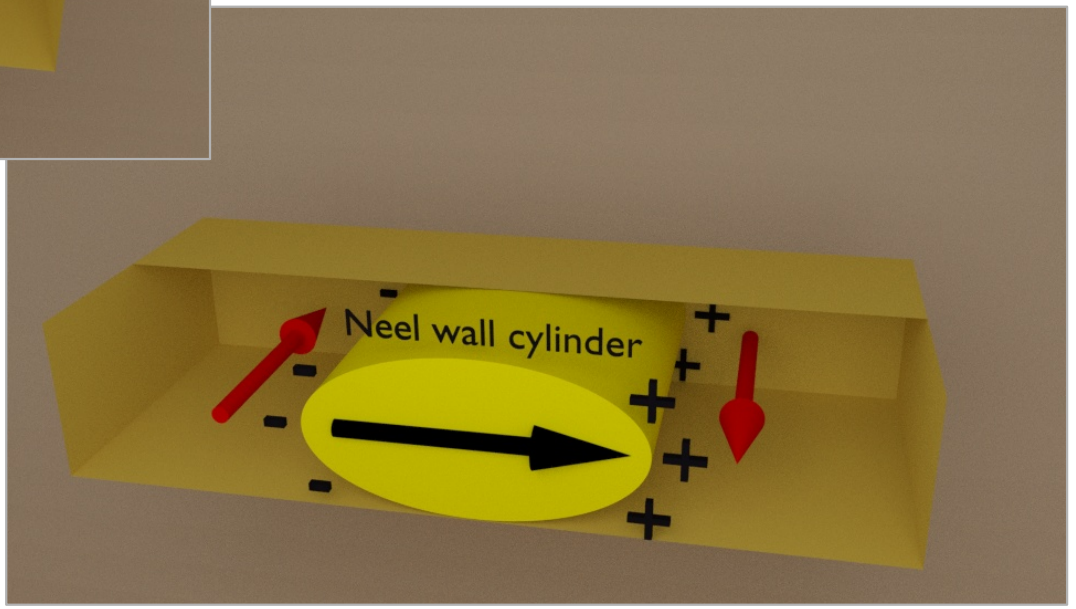

Domain walls in thin films

- Magnetic films are defined as **thin** if their thickness is comparable with Bloch wall width [1].

- A Bloch and Néel walls can be approximated by an infinite elliptical cylinder, of height equal to the thickness of the film [1,2], placed between regions of opposite magnetization.
- Within the cylinder demagnetizing field is created (N is taken from general expression**):

$$H_d = M_e N = \frac{M_e w}{w + t}, \qquad M_e \text{ - effective magnetization of the wall (see below)}$$

t- film thickness
w -wall width

- Magnetostatic energy associated with that field is:

$$E_d = \frac{1}{2}\mu_0 N M_e^2 = \mu_0 \frac{M_e^2 w}{w + t} \qquad (1)$$

- The spin angle within the wall is supposed to change according to the expression*:

$$\phi = \pi(x/a) \quad for \quad -a/2 \le x \le a/2$$

a - wall width, φ – the angle between the magnetization and a direction in the plane of the wall and perpendicular to the plane of the film

- For a given φ(x) dependence the anisotropy energy density (averaged along the wall width) is:

$$E_A = \frac{1}{a}\int_{-a/2}^{a/2} K\cos^2[\pi(x/a)]dx = \frac{1}{2}K$$

*this is just an assumption, without proof; S. Middelhoek, J. Appl. Phys. 34, 1054 (1963)
** Eq. 3.23 in [1]; in numerator we have the shorter axis of the ellipsoidal cross section of the cylinder

Domain walls in thin films

- To find the effective magnetization of the Bloch wall in very thin films* (t≪w) we calculate the magnetostatic energy of the wall in its own demagnetizing field:

$$E_d = \frac{\mu_0}{a}\int_{-a/2}^{a/2} 1 \cdot M_S^2 \cos^2\left[\pi\left(\frac{x}{a}\right)\right] dx = \frac{1}{2}\mu_0 M_S^2$$

demag factor for thin film

- Comparing this with Eq.(1) for t≪w we obtain:

$$E_d = \mu_0 \frac{M_e^2 w}{w+t} \approx \mu_0 M_e^2$$

$$M_e = \frac{M_s}{\sqrt{2}}$$

The Bloch wall can be approximated by the infinite cylinder if we decrease magnetization by a factor of 0.7... It is further assumed that this is true for thicker films too.

- The total energy of the wall (per unit area) is obtained by summing exchange, magnetocrystalline and stray field energy densities (volume energy densities are multiplied by wall thickness):

$$\gamma = A\left(\frac{\pi}{a}\right)^2 a + \frac{1}{2}K a + \mu_0 \frac{M_e^2 a}{a+t} a \qquad \cos(x) = 1 - \frac{x^2}{2} + \ldots$$

•The energy is minimized with respect to **wall width *a*** and that value is inserted back in the expression for the energy.

S. Middelhoek, J. Appl. Phys. 34, 1054 (1963)

*we can then use the approximation that the demag field at *x* depends only on magnetization at x.

Domain walls in thin films

- The same kind of approximate calculations can be performed for Néel wall
- The wall is represented by the cylinder as in the case of Bloch wall, but it is now flattend; as a consequence the demagetization coefficient changes:

$H_d = M_e N = \frac{M_e t}{w + t}$, M_e - effective magnetization of the wall (see below)

- It is assumed that the effective magnetization is the same as in the case of “Bloch cylinder”.
- For Néel wall the expression for the total energy is then:

$$\gamma = A\left(\frac{\pi}{a}\right)^2 a + \frac{1}{2} K a + \mu_0 \frac{M_e^2 t}{a + t} a$$

← the only difference between Néel and Bloch walls within the present model

- The energy and domain wall width dependence on film thickness can be obtained numerically. Here the exemplary *Mathematica* code:

```
A=1;
mi0=1;
K=1;
Ms=1;
energyNeel[a_,t_]=A (Pi^2/a)+0.5 a K+(0.5 mi0 Ms^2 a t/(a+t));
tmax=40;
ilepunktow=201;
w=Table[{t//N,FindMinimum[energyNeel[x,t],{x,2}][[2,1,2]]},{t,0,tmax,tmax/(ilepunktow-1)}];
ListPlot[w,Joined->False] (*wall width versus film thickness*)
energiavsthickness=Table[{i tmax/(ilepunktow-1)//N,energyNeel[w[[i,2]],i tmax/(ilepunktow-1)]},{i,1,ilepunktow,1}];
ListPlot[energiavsthickness,Joined->False](*wall energy versus film thickness*)
```


S. Middelhoek, J. Appl. Phys. 34, 1054 (1963)

Energy of Bloch and Néel wall

- In case of thin films the most important difference between those kinds of domain walls is their dependence on film thickness:

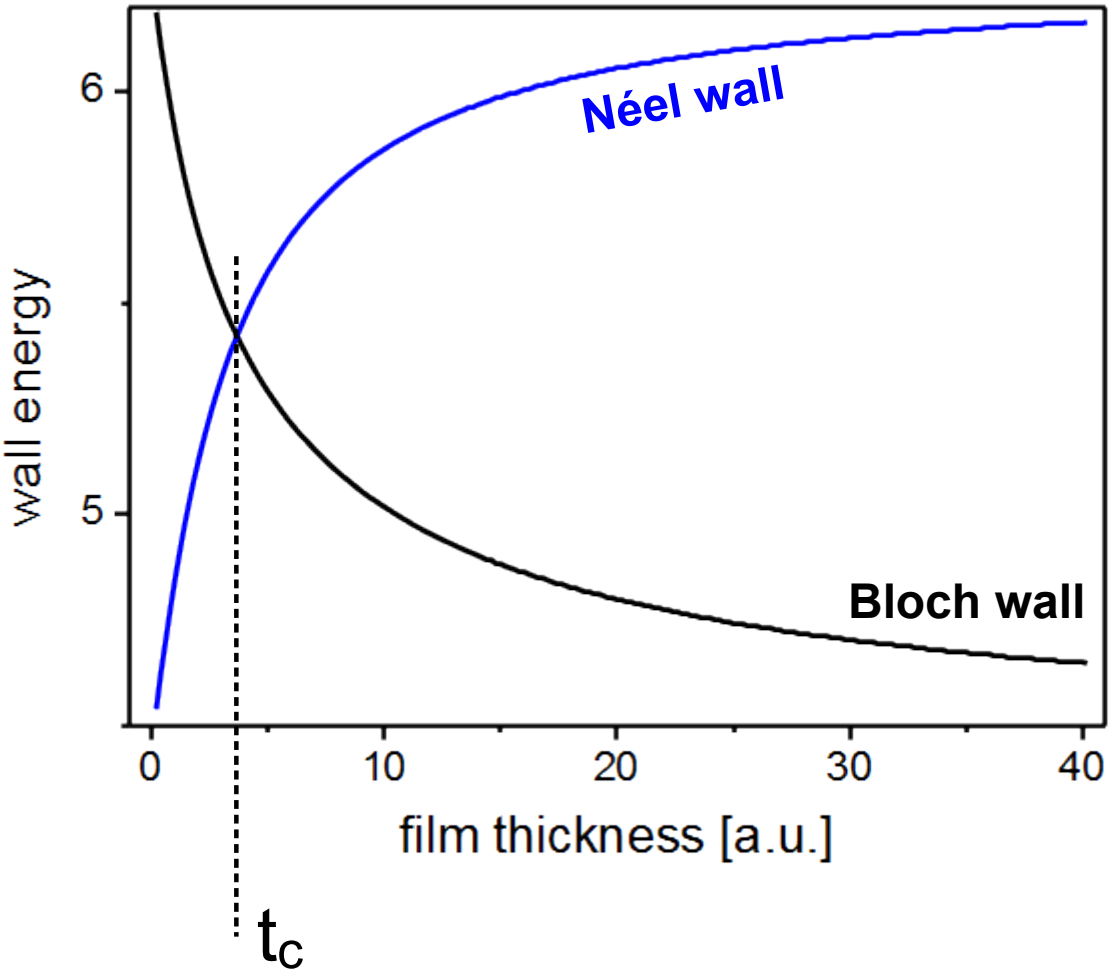

- At certain critical thickness the energy of Néel wall becomes less than the energy of Bloch wall
- The Néel walls are favored in thin easy-plane* anisotropy films
- In thin perpendicular anisotropy films Bloch walls may be energetically favored

*
- easy-plane anisotropy – the energy does not depend on the orientation within the plane
- in-plane anisotropy - the energy does depend on the orientation within the plane

S. Middelhoek, J. Appl. Phys. 34, 1054 (1963)

Energy of Bloch and Néel wall

- The same model predicts the thickness dependence of domain wall width:

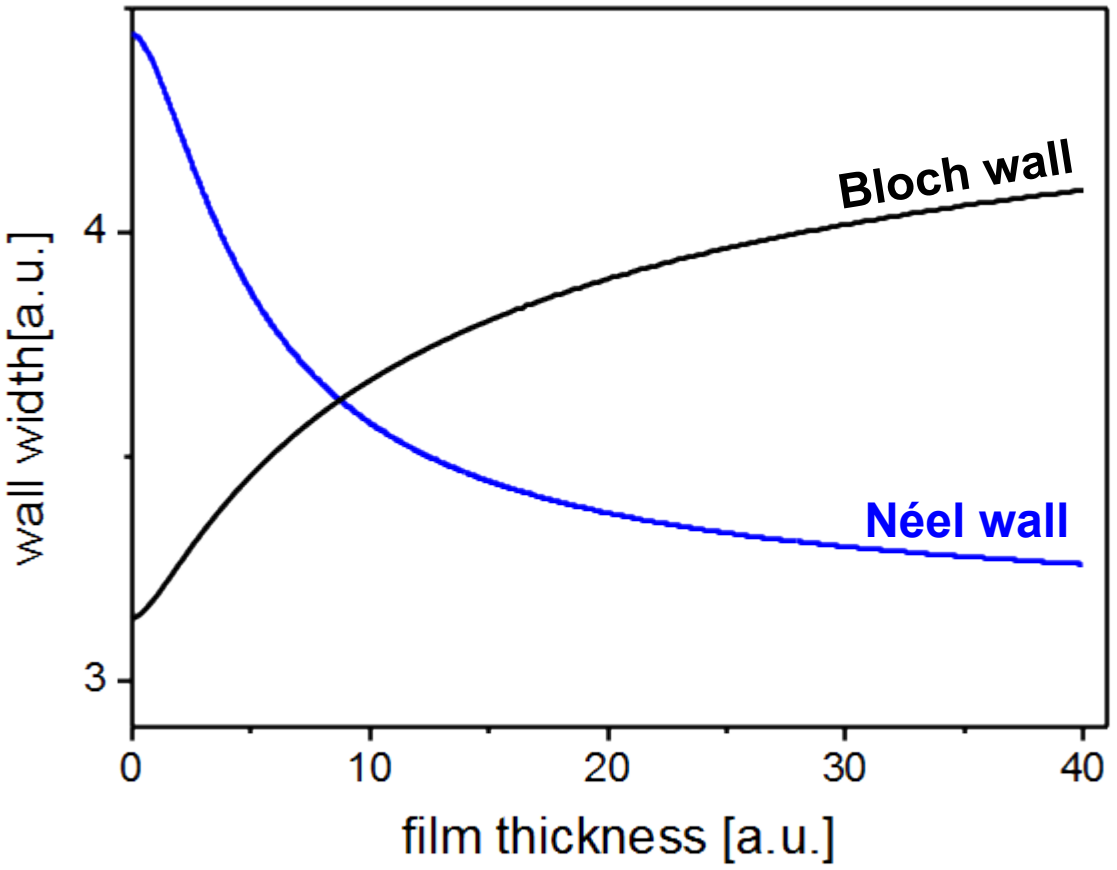

- In permalloy $\sqrt{A/K_d}$ is about 5 nm [1]

- Néel walls are characterized by core region with dipolar charge pattern (see 13 slides back) and long tails

- The more elaborate calculations give that core width can be expressed as:

$$W_{core} = 2\sqrt{\frac{A}{(K_u + K_d)(1 - c_o^2)}}$$

, where c_0 is a cosine of the spin angle corresponding to core-tail boundary.

- **The spin angle of Néel wall is, similarly to Bloch wall, field dependent**

- With increasing K_d core width decreases and tails get longer

Energy of Bloch and Néel wall

- The critical thickness of the Bloch-Néel wall transition is of the order of tens of nanometers:

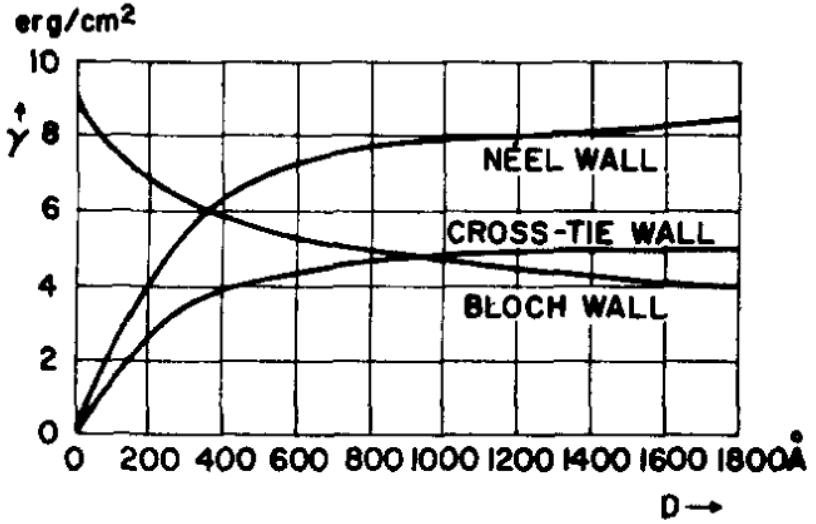

FIG. 1. Energy per unit area of a Bloch wall, a Néel wall and a cross-tie wall as a function of the film thickness [$A = 10^{-6}$ ergs/cm, $M_s = 800$ G, and $K = 1000$ ergs/cm³].

- Other types of walls exist which can have lower energy then Bloch or Néel walls depending on thickness, external field value etc.:

-cross-tie walls

-asymmetric Bloch and Néel walls

S. Middelhoek, J. Appl. Phys. 34, 1054 (1963)

Cross-tie walls

- At intermediate thicknesses cross-tie walls exists
- They are composed of alternating regions of Bloch and Néel-like transitions
- In permalloy films they are observed for thickness
- range from 30 to 90 nm
- Schematic view of cross-tie wall:

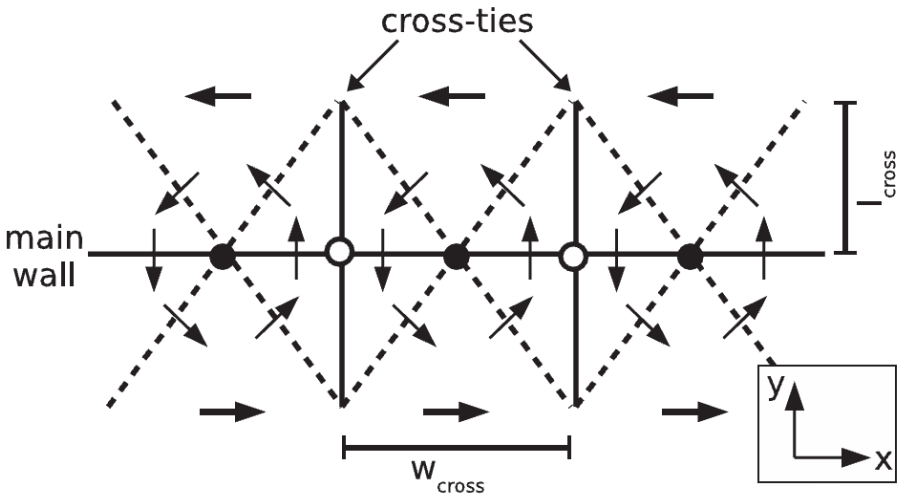

Fig. 1: Schematic of a cross-tie domain wall.

N. Wiese et al., EPL 80, 57003 (2007)

- Note the change of the cross-ties spacing as a function of the effective anisotropy (introduce by bending of the film – stress anisotropy)

S. Middelhoek, J. Appl. Phys. 34, 1054 (1963)

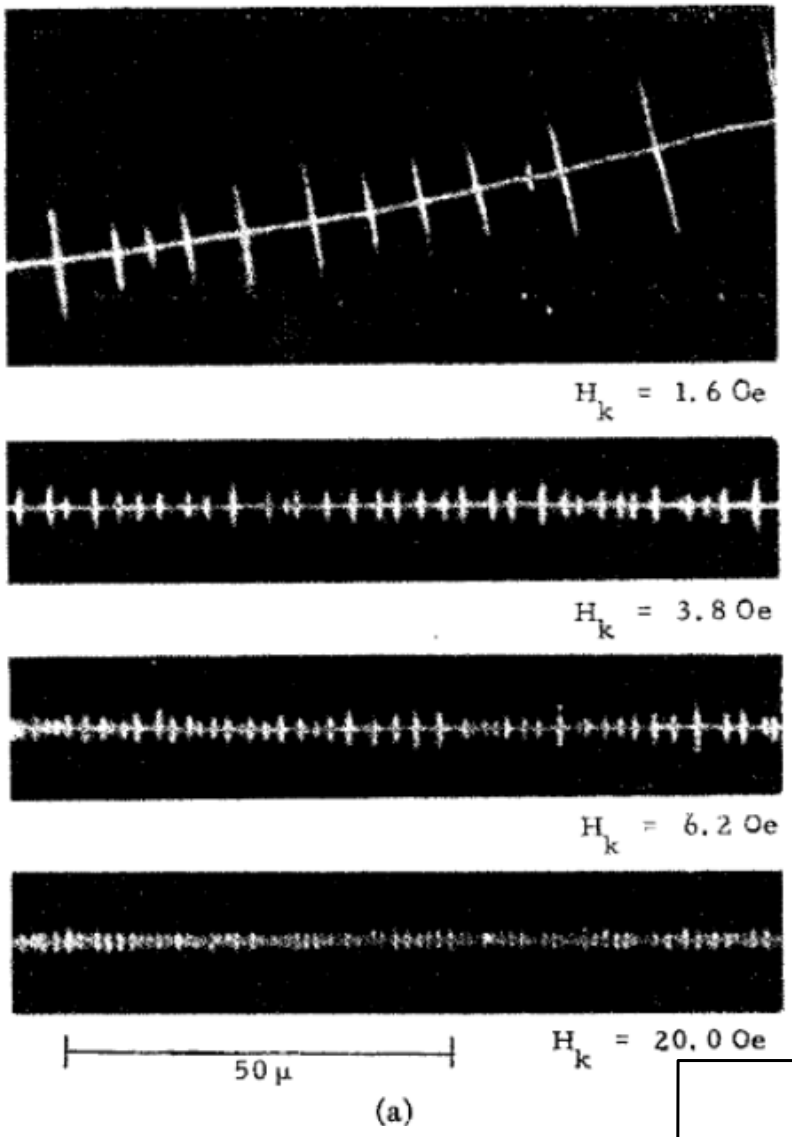

Bitter patterns of a cross-tie wall for different anisotropy fields H_K

Cross-tie walls

- The inner structure of the cross-tie walls can be resolved with contemporary imaging methods.

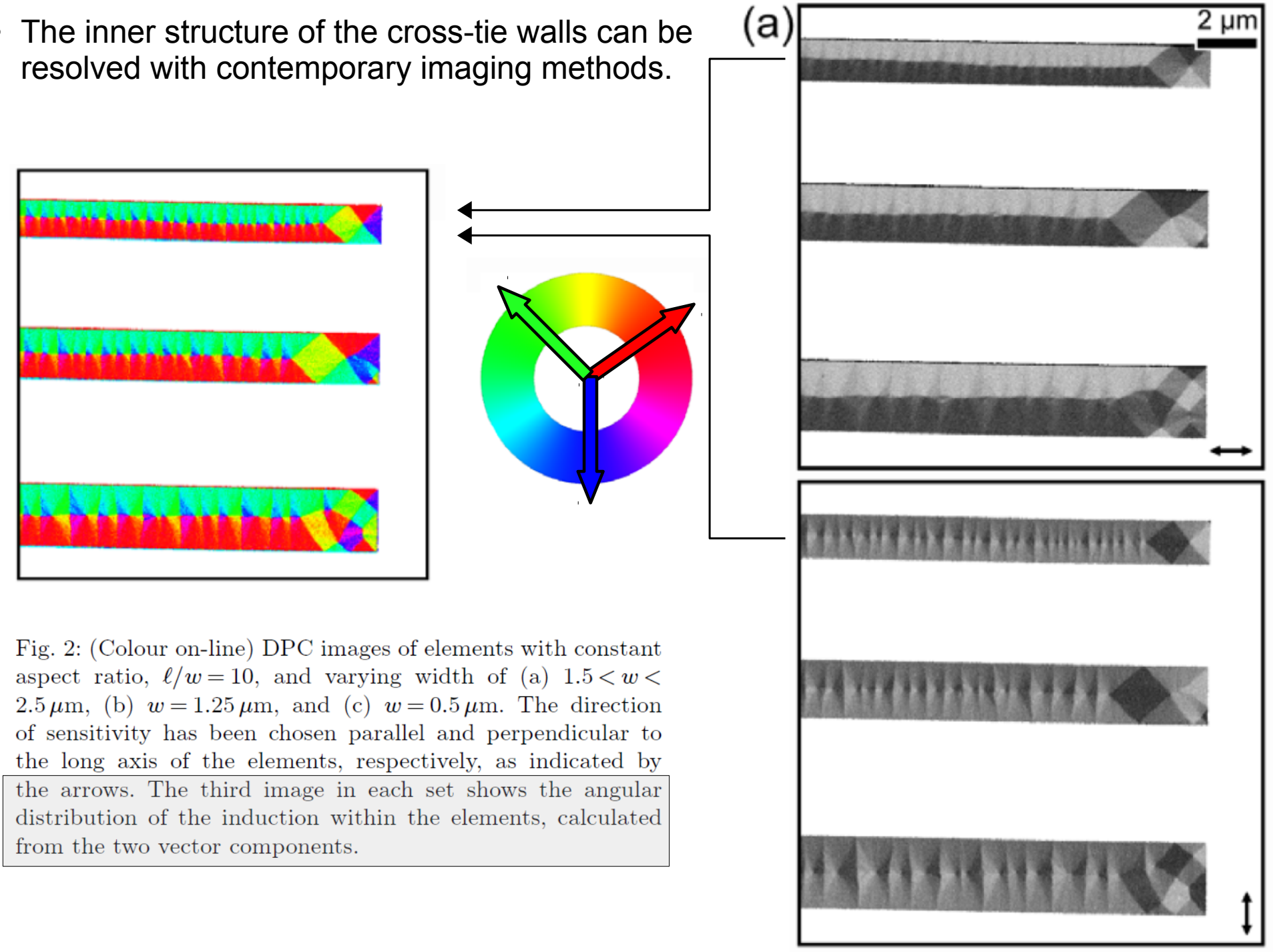

Fig. 2: (Colour on-line) DPC images of elements with constant aspect ratio, $\ell/w = 10$, and varying width of (a) $1.5 < w < 2.5\,\mu$m, (b) $w = 1.25\,\mu$m, and (c) $w = 0.5\,\mu$m. The direction of sensitivity has been chosen parallel and perpendicular to the long axis of the elements, respectively, as indicated by the arrows. The third image in each set shows the angular distribution of the induction within the elements, calculated from the two vector components.

N. Wiese et al., EPL 80, 57003 (2007)

Cross-tie walls

- The cross-tie wall images obtained from Lorentz microscopy* confirm the predicted structure of the transition region:

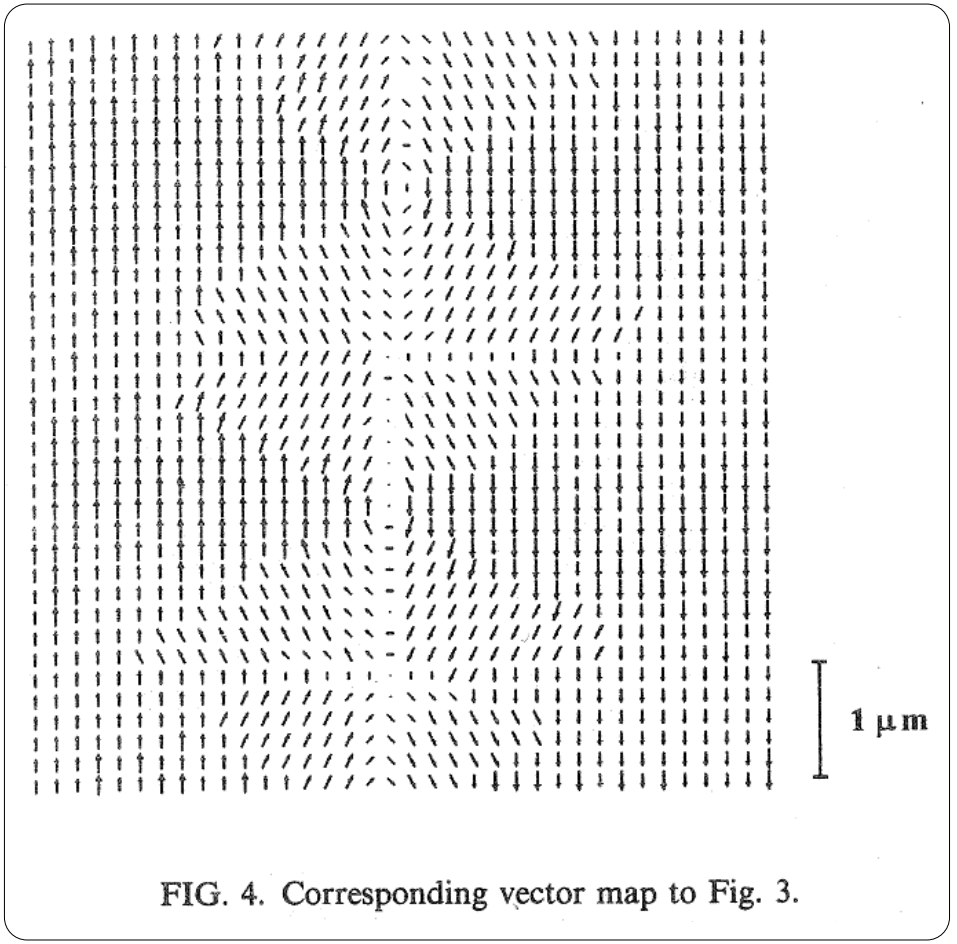

FIG. 4. Corresponding vector map to Fig. 3.

R. Ploessl et al., J. Appl. Phys. 73, 2447 (1993)

Cross-tie structure of the evaporated 60 nm thick permalloy film (*from Lorentz electron microscopy image*).

*detects the force acting on imaging electrons due to magnetic field

Asymmetric walls

- In some cases asymmetry of the spin angle in domain wall may result in **stray-field free** domain walls in thin films:

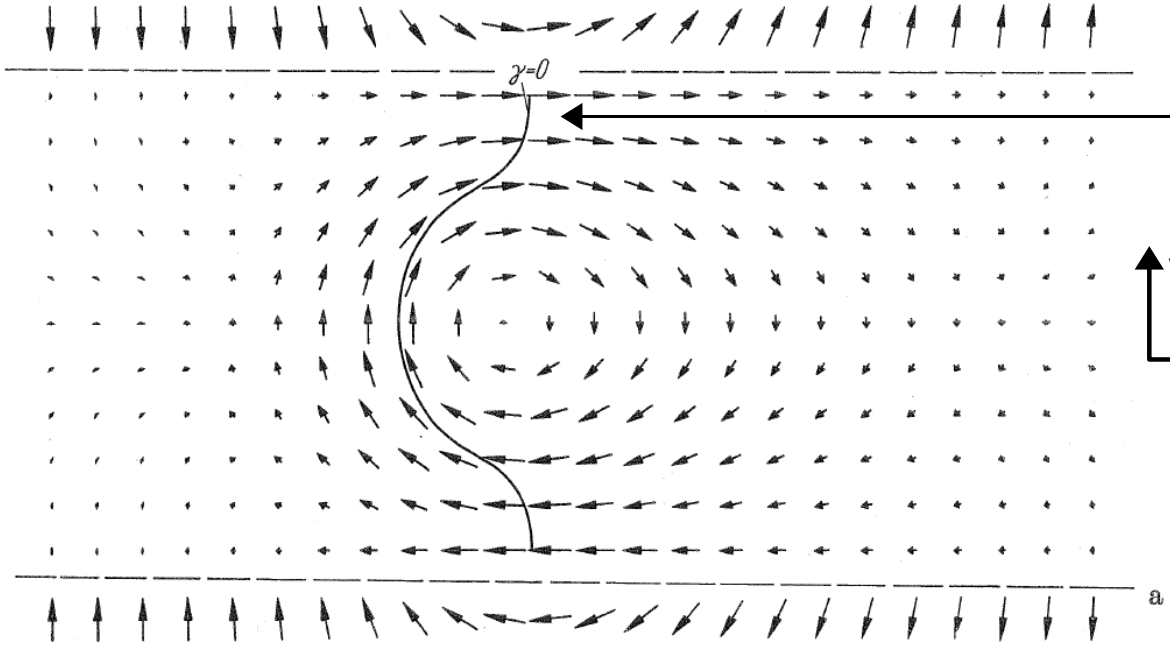

The contour line indicates the "center" of the wall, i.e. the surface on which z-component of magnetization passes through zero

A. Hubert, phys.stat.sol. 38 699(1970)

4. Vector diagrams of asymmetric Bloch walls. These models are more or less valid for all film thicknesses.
a) $h = 0$

- In "normal" walls "center" of the wall is planar
- Similarly stray-field free configurations can be obtained for Néel walls [1].

Asymmetric walls

- Depending on film thickness and external field value various kinds of domain wall are energetically favored:

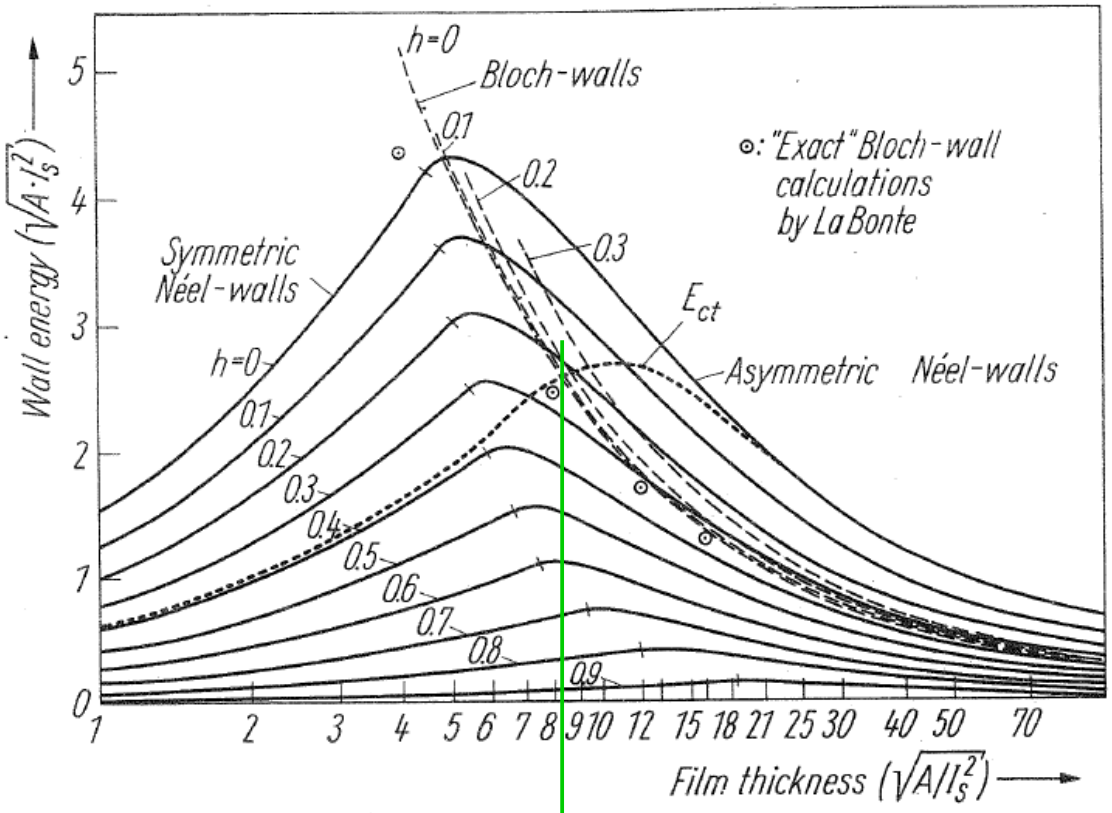

Fig. 1. The total wall energies per unit wall surface as a function of film thickness. Parameter is the reduced applied field $h = H\,I_s/(2\,K)$. $K/I_s^2 = 1/640$

$$h = H\frac{\mu_0 M_S}{2K}$$

an example: critical thickness for a Bloch vs. symmetric Néel wall transition for field H=0.2

- Bloch walls are only stable compared to Néel walls up to reduced field h=0.3.

A. Hubert, phys.stat.sol. 38 699(1970)

360º walls

- In thin films two Néel walls of the opposite rotation sense (unwinding walls) attract each other each other – because they generate opposite charges in their overlapping tails [1].
- In thin films two Néel walls of the same rotation sense (winding walls) repel each other:

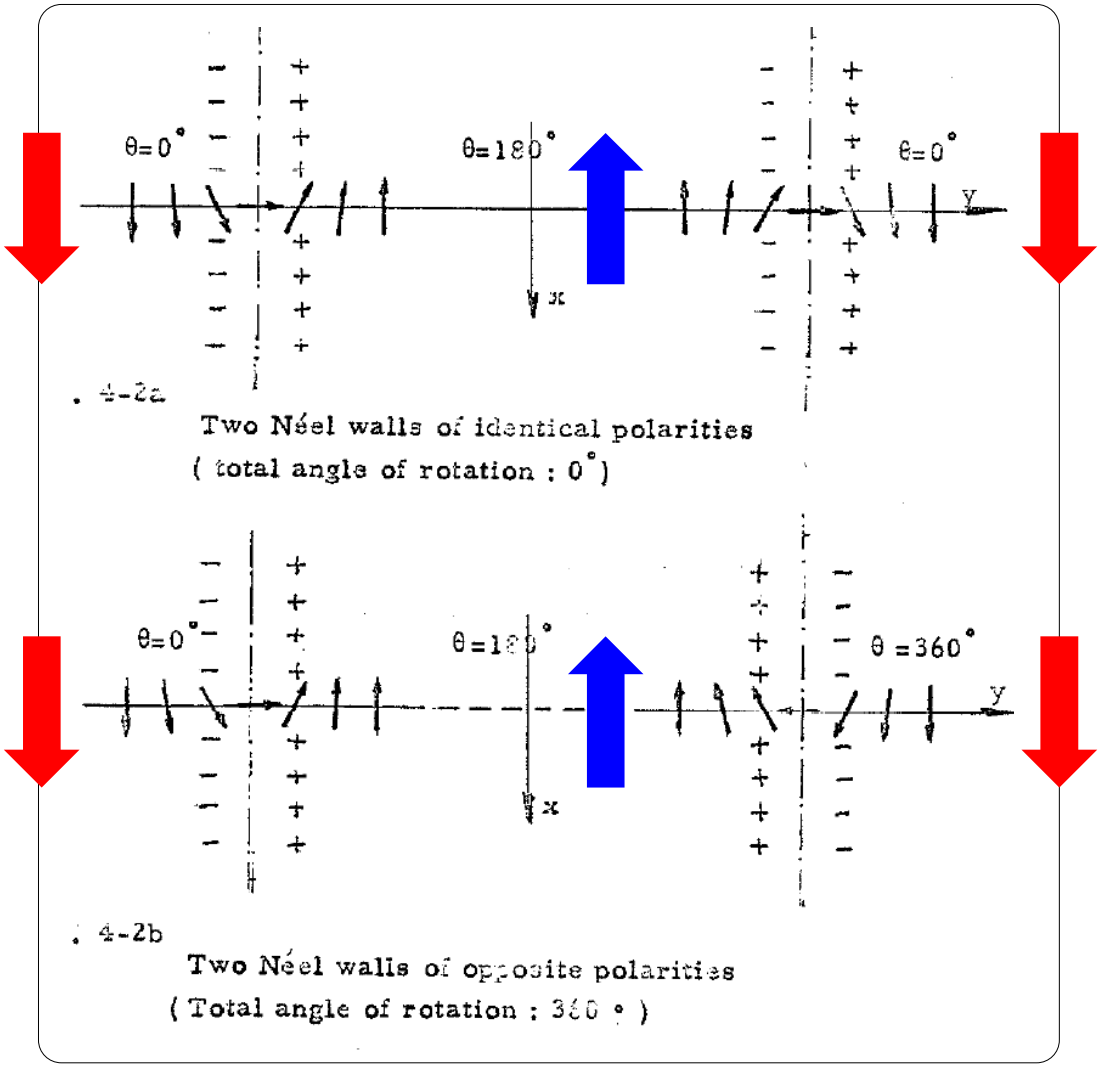

- When to unwinding walls meet they can annihilate
- If the winding walls are pressed together by the action of the external field energetically disfavoring the magnetization direction within the walls (blue arrow) they create so called 360º wall.
- The 360º wall can be annihilated only in large fields [1].
- In permalloy films of 50 nm thickness Néel walls interact over distances at least **0.1mm!** (2000 times the thickness)

R.C. Collette 1964, dissertation, Pasadena 1964

360º walls

- From the point of view of applications 360º walls should be avoided as they may reduce the reproducibilty of switching events*

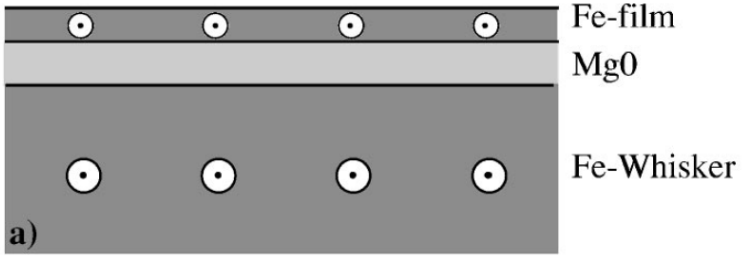

The domain structure in Fe layer and whisker is the same due to magnetostatic interactions

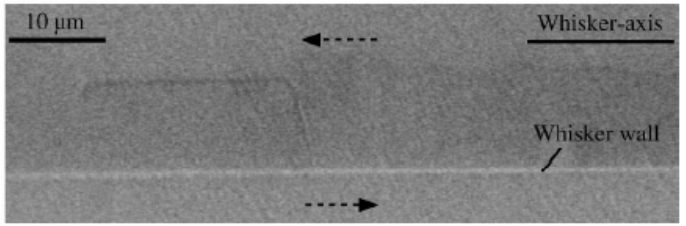

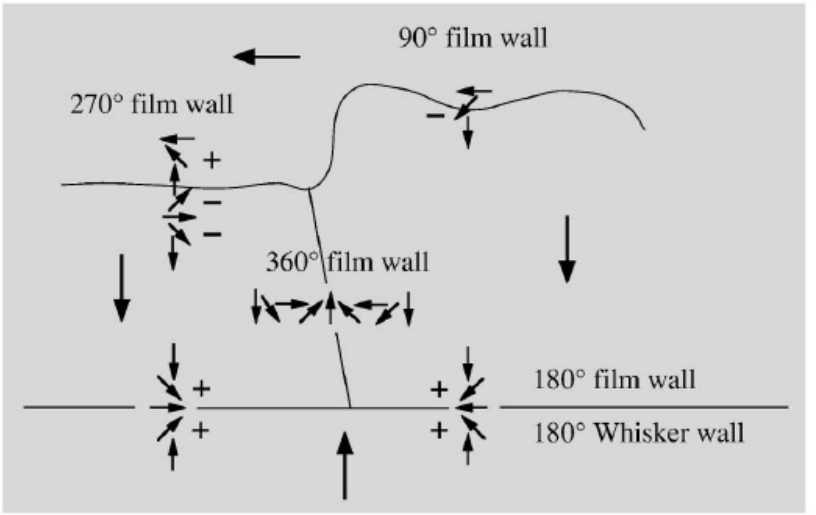

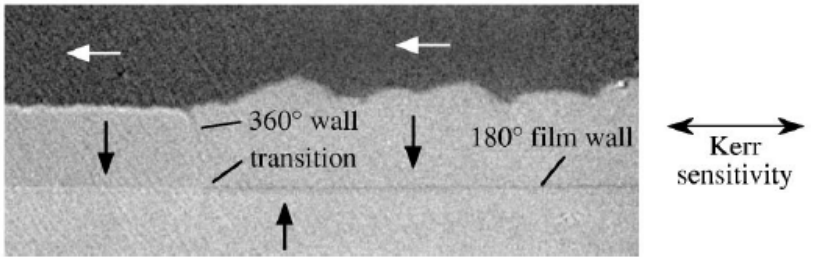

FIG. 5. (a) Domain pattern in the iron film, containing 360° domain walls. The formation of 360° walls is shown by film-selective images in (b) and (c). The domain state of (c) is selectively imaged in (d) by whisker. Wall segments of certain polarities are responsible for the formation of 360° walls as explained schematically in (e). The expected change in chirality of the 180° film wall is verified in (f).

R. Schäfer et al., PHYSICAL REVIEW B **65**, 144405 (2002)

*C. B. Muratov and V. V. Osipov J.Appl. Phys. **104**, 053908 (2008)

360° walls

- Domain walls can be generated by the proper external field sequence:

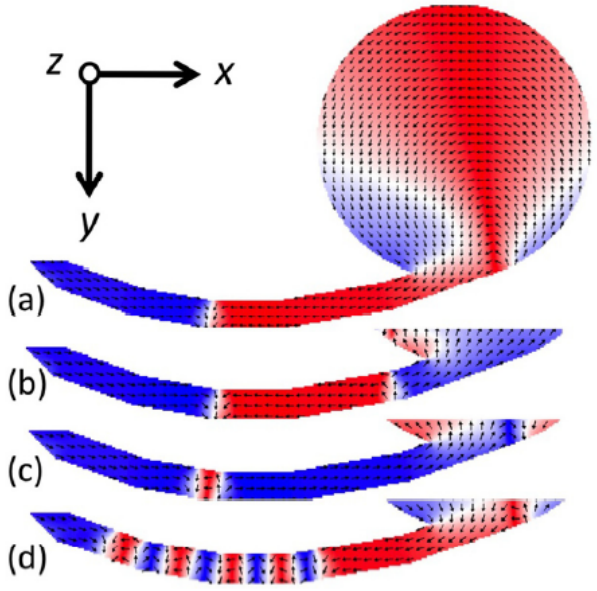

FIG. 1. (Color online) OOMMF model of formation of 360DW in a wire attached to a circular pad. (a) After 239 kA/m saturation along y, a 180DW formed in the wire, shown at remanence. (b) A further field of −4.0 kA/m along y produced a second 180DW. (c) The remanent state showing a 360DW. (d) Repeated alternating field of magnitude 9.5 kA/m along y generated multiple domain walls. Red and blue (or greyscale shading) represent the sign of the x-component of the magnetization.

other sample- two 180° walls

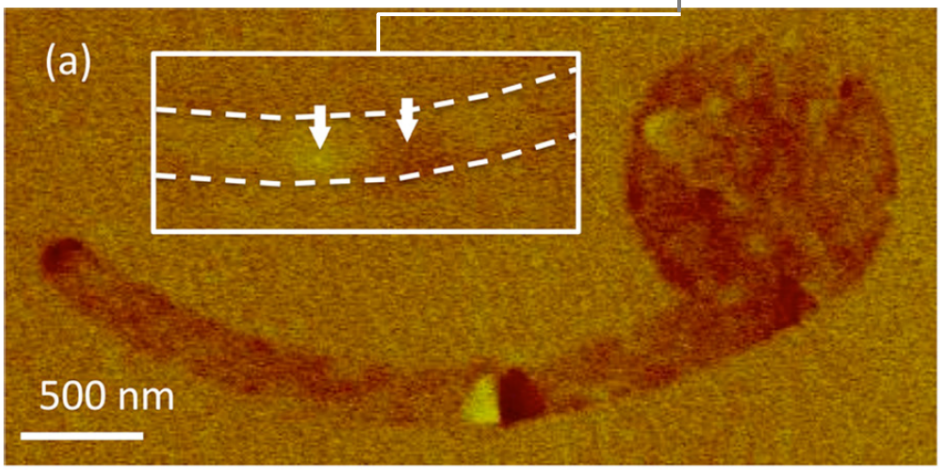

imaged at a tip height of **20 nm**

5nm thick Co structure
$4\times4\times5$ nm^3 micromagnetic cells

Field sequence:
- 239 kA/m saturation along y- direction
- remanence - 180° wall generated
- -15.9 kA/m field produced the second 180° wall
- remanence – two 180° walls meet to create 360° wall

- Results of micromagnetic simulations are confirmed with Magnetic Force Microscopy images

Youngman Jang etal., Aplied Physics Letters 100, 062407 (2012)

540^o walls

- Inserting a consecutive 180^o wall to the wire with 360^o wall can create 540^o wall:

Appl. Phys. Lett. **100**, 062407 (2012)

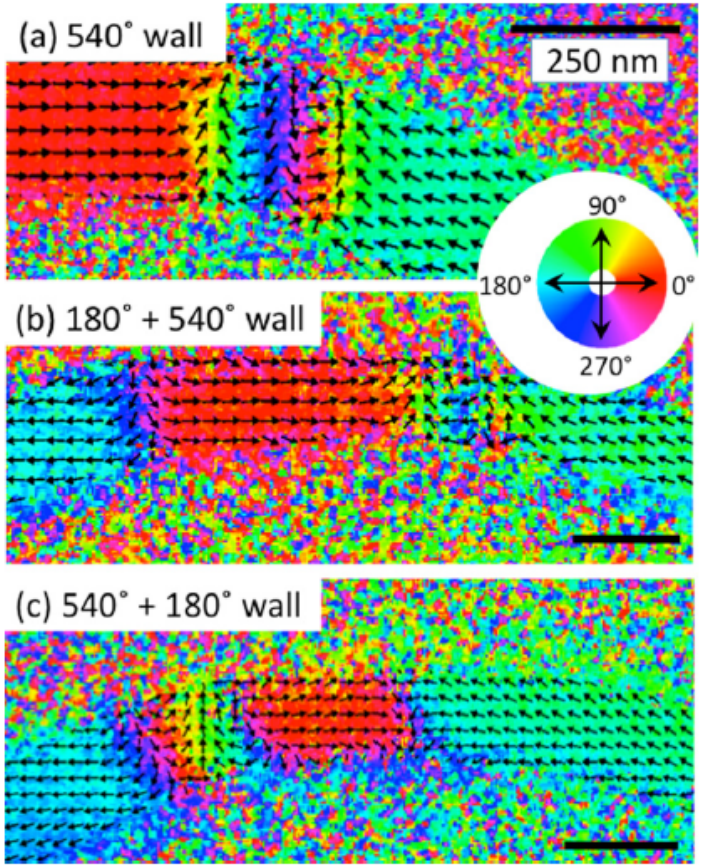

FIG. 4. (Color online) (a) SEMPA image of a 540DW. (b) SEMPA image after injecting an additional 180DW. (c) A 540DW of opposite sense to that of (a) adjacent to a 180DW. Magnetization directions are indicated on a color wheel. The uncertainty in the SEMPA angular data is 7.4° (one standard deviation). Scale bars are 250 nm.

SEMPA* images suggest the possibility of producing higher order walls – with nπ rotation

- 360^o walls have well-defined structure and persist over wide field range

*SEMPA-scanning electron microscopy with polarization analysis

Youngman Jang etal., Aplied Physics Letters 100, 062407 (2012)

Magnetic whiskers

- Due to almost **perfect crystallinity** whiskers are ideal for the investigations of simple domain structures [1].
- Whiskers are usually grown from vapor phase by chemical reactions
- Process parameters (temperature, pressure etc.) control the sizes, type and the perfection of the whiskers
- The whiskers can be up to several millimeters in size
- Domain observation is possible from all sides [1].
- Typical domain structure of whisker:

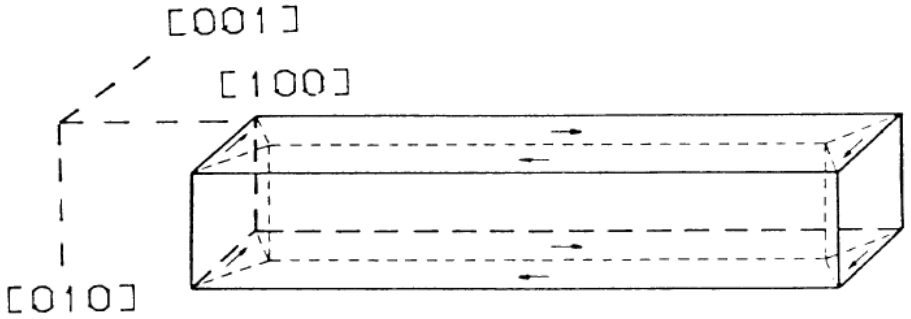

FIG. 1. Landau domain structure of an iron whisker grown in a ⟨100⟩ crystallographic direction and bounded by {100} faces.

J. Phys. D: Appl. Phys. **45** (2012) 085001

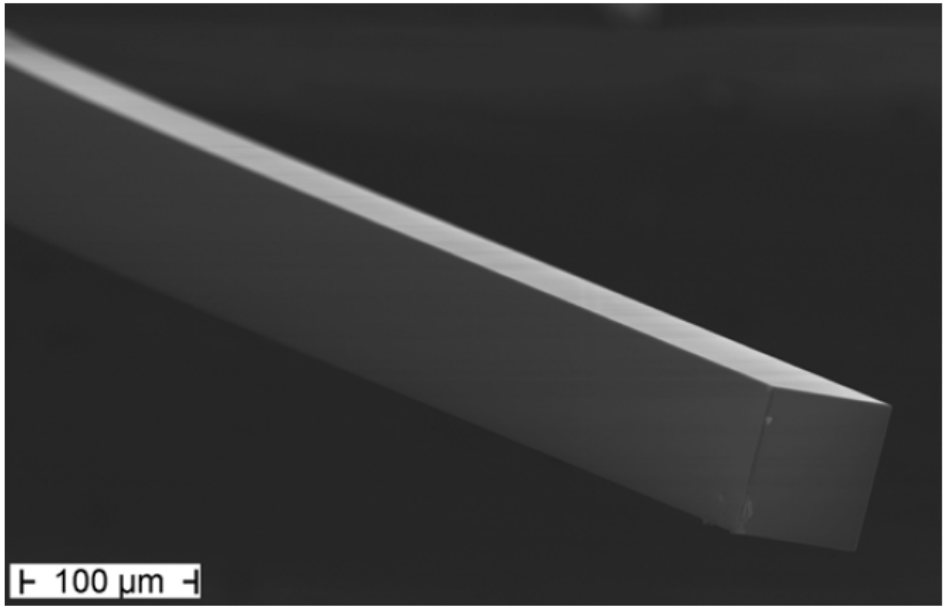

M. Langosch, H. Gao, U. Hartmann

Figure 1. SEM image of an iron whisker with ⟨1 0 0⟩ growth direction.

U. Hartmann, Phys. Rev. B **36**, 2331 (1987)

Magnetic whiskers

- Due to almost **perfect crystallinity** whiskers are ideal for the investiagtions of simple domain structures [1].

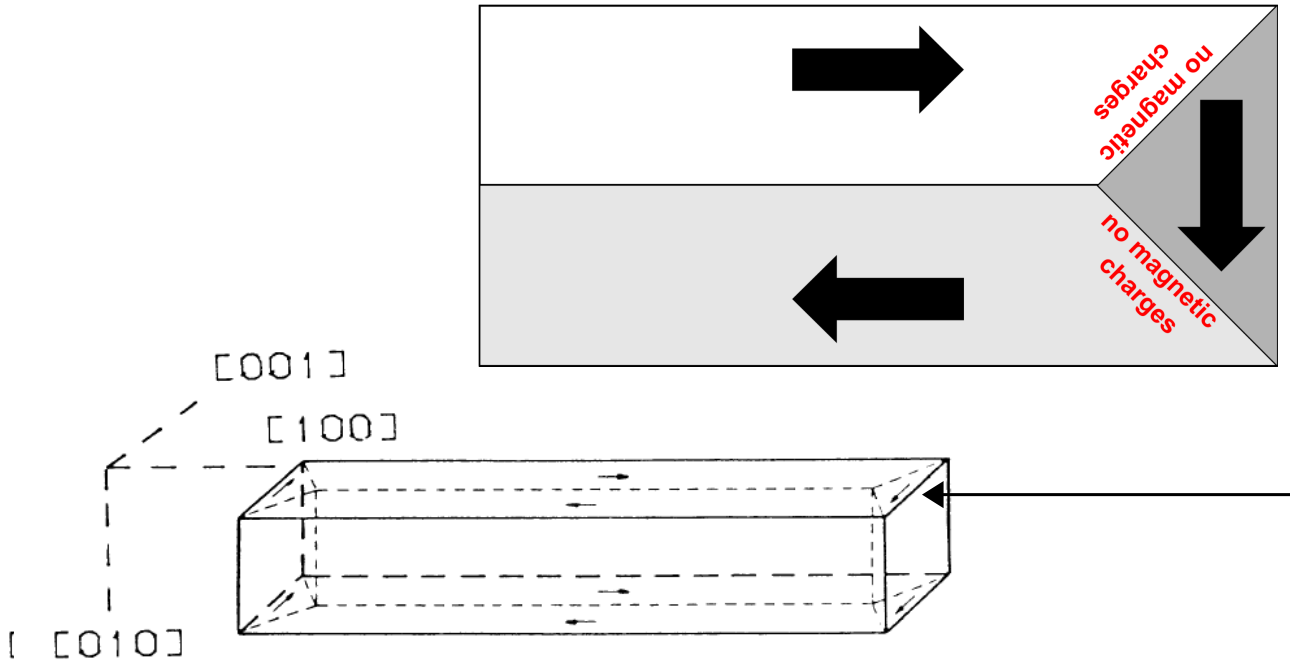

perfect **closure domains** produce no magnetic fields

FIG. 1. Landau domain structure of an iron whisker grown in a ⟨a⟨100⟩ crystallographic direction and bounded by {100} faces.

U. Hartmann, Phys. Rev. B **36**, 2331 (1987)

Magnetic whiskers

- **Brown's coercive paradox** – coercive fields predicted by the early (1940s) calculations hugely overestimated the experimental results.
- Brown predicted, assuming ellipsoidal shape of the sample, that the reversal (coercive) field should be:

$$H_r > \frac{2K}{\mu_0 M_s} - N_d M_s$$

- In whiskers "*huge demagnetizing fields associated with a uniformly magnetized corner cause the formation of closure domains (...) which remain even during the overall magnetization of the whisker.*" (U. Hartmann).

- The whisker electropolished in $Cr0_3$ glacial acetic acid show greatly increased coercive field and hysteresis characteristic for single-domain particles.

Polished whiskers have much higher coercive fields

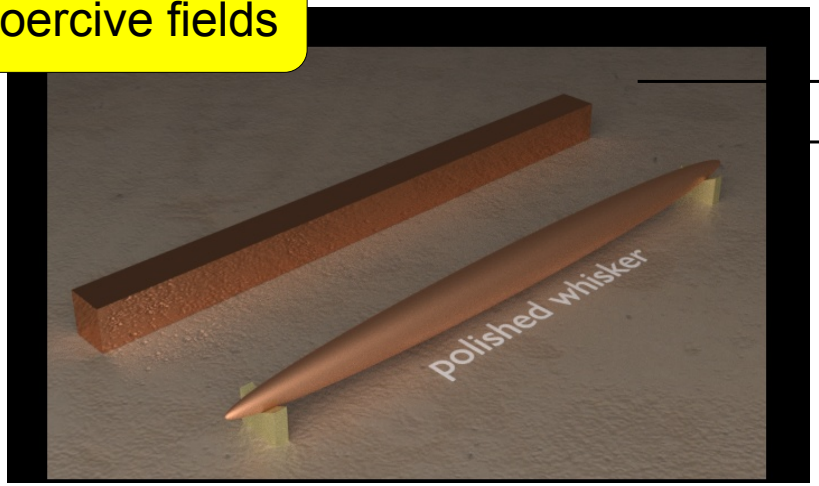

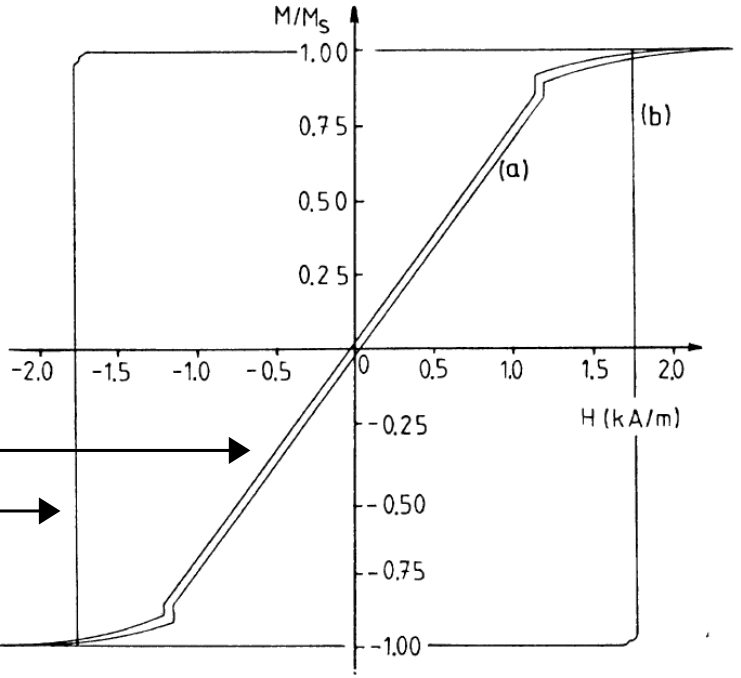

FIG. 2. (a) Magnetization curve of a whisker in the as-grown state, (b) after smoothing of the whisker tips.

U. Hartmann, Phys. Rev. B **36**, 2331 (1987)

Magnetic wires

- In contrast to whiskers they do not have, in general, perfect structure
- Amorphous magnetic wires find applications in sensors
- Due to the high curvature of the surface modifications of standard domain imaging methods must be employed. On of the methods is the magneto-optical indicator film (MOIF) microscopy:

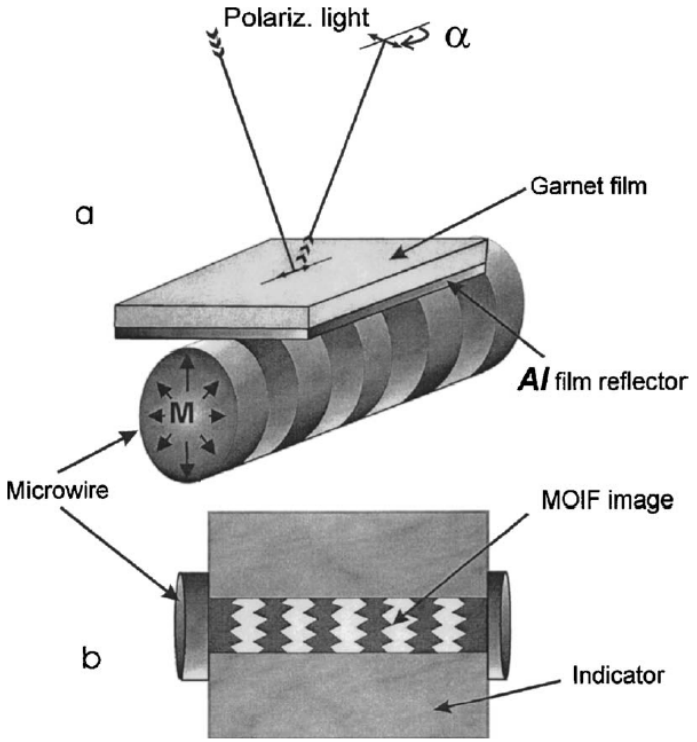

FIG. 1. Schematic picture showing the experimental setup configuration (a) and the MOIF images from Fe-rich wire (b).

- Magnetic moments within garnet indicator film with high Verdet constant are influenced by the stray fields coming from the surface of the wire
- The changes in magnetic structure of the indicator film are detected by the Faraday effect which is sensitive to the magnetization component parallel to incident light.

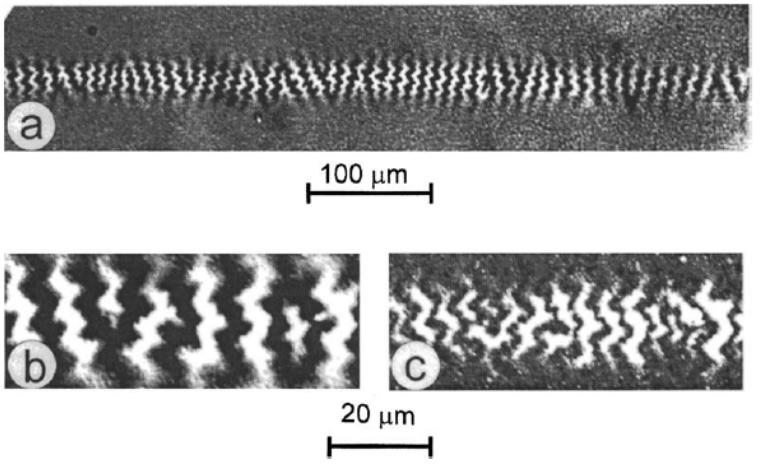

FIG. 2. Magneto-optical contrast of the magnetization distribution on the surface of the Fe-rich wire (a, b) and (c) MOIF image of the domain walls in the region as indicated in (b).

Yu. Kabanov, A. Zhukov, V. Zhukova, and J. Gonzalez, Applied Physics Letters **87**, 142507 (2005)

Magnetic wires

- In contrast to whiskers they do not have, in general, perfect structure
- Amorphous magnetic wires find applications in sensors
- Due to the high curvature of the surface modifications of standard domain imaging methods must be employed. On of the methods is themagneto-optical indicator film (MOIF) microscopy.
- Labirynth-like *open domain structure** is present in the wire
- In Fe-rich wires ($Fe_{77.5}B_{15}Si_{7.5}$), with **positive magnetostrictions, the magnetic moments are perpendicular to the surface** in the regions close to surface and the domains are separated by 180° walls.
- In Co-rich wires ($Co_{72.5}B_{15}Si_{12(?)}$), with negative magnetostriction, magnetic moments are parallel to the surface of the wire
- The core of the wire is magnetized approximately along the wire axis with domains no less than 0.5mm in size.

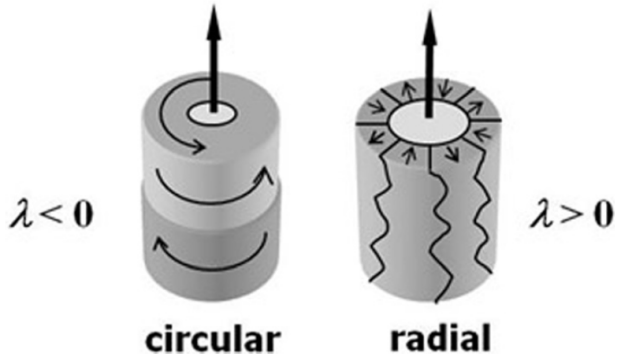

FIG. 1. Domains with circular and radial magnetization.

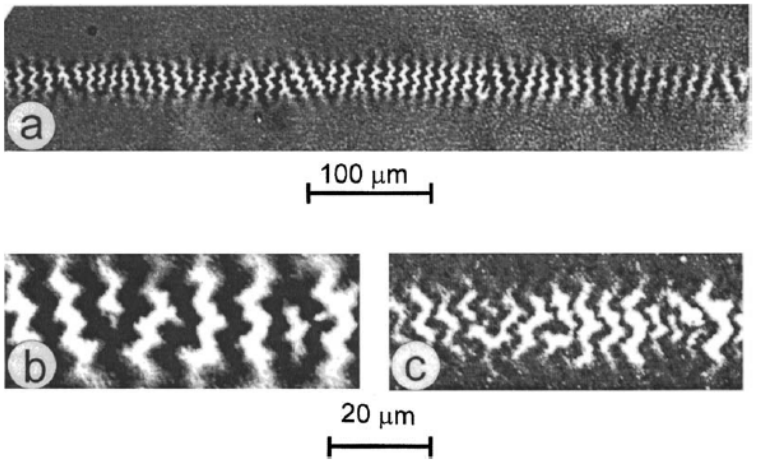

FIG. 2. Magneto-optical contrast of the magnetization distribution on the surface of the Fe-rich wire (a, b) and (c) MOIF image of the domain walls in the region as indicated in (b).

image from: N. N. Orlova, A. S. Aronin, S. I. Bozhko, Yu. P. Kabanov, and V. S. Gornakov, J. Appl. Phys. 111, 073906 (2012)

*that is without closure domains
Yu. Kabanov, A. Zhukov, V. Zhukova, and J. Gonzalez, Applied Physics Letters **87**, 142507 (2005)

Domain wall in external magnetic field – Walker limit

- The velocities of domain walls are highly unlinear functions of the applied magnetic field.
- In “small fields”, up to the so called **Walker field H_W**, the velocity of the wall is approximately a linear function of the applied field.
- Above the critical field the velocity of the wall may fluctuate
- In samples of limited dimensions (wires, patterned media, etc.) the orientation of easy axes with respect to sample surfaces influences the character of velocity-field dependence [10].

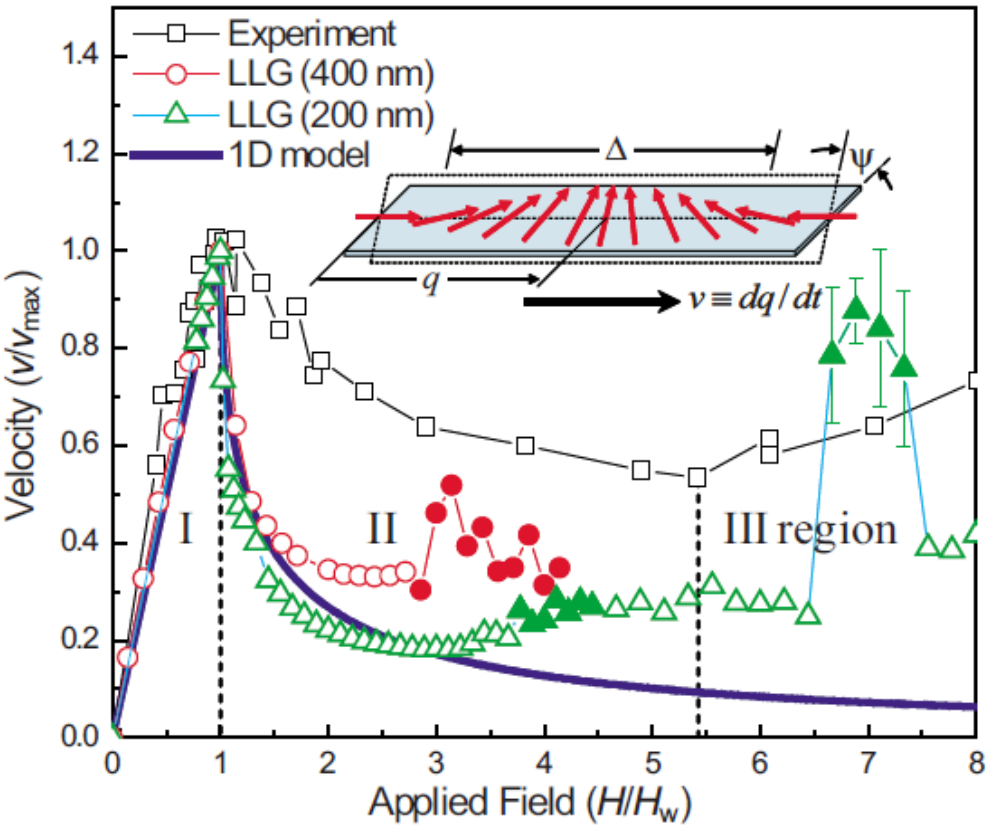

FIG. 1. (Color online) Measured and simulated DW velocity [normalized to $v_{max} \equiv v(H_W)$] as a function of applied field (normalized to the Walker field H_W). Walker breakdown occurs at $H=H_W$ corresponding to $\psi=\pi/4$. (Inset) Schematic description of the spin distribution within a propagating transverse DW showing tilt angle ψ and wall width Δ. Solid symbols for LLG simulations designate onset of noise in simulated velocity described later in text.

Jusang Yang, Corneliu Nistor, G. S. D. Beach, and J. L. Erskine, Phys. Rev. B **77**, 014413 (2008)

Domain wall in external magnetic field – Walker limit

- If the external field is applied parallelly to the straight Bloch wall the torque is exerted only on the spins within the wall (neglecting the infinite extent of the wall - see lecture 6).
- The torque forces precession of moments (see LLG equation – next lecture or lecture 7/2012) giving demagnetizing field component perpendicular to the wall [11].

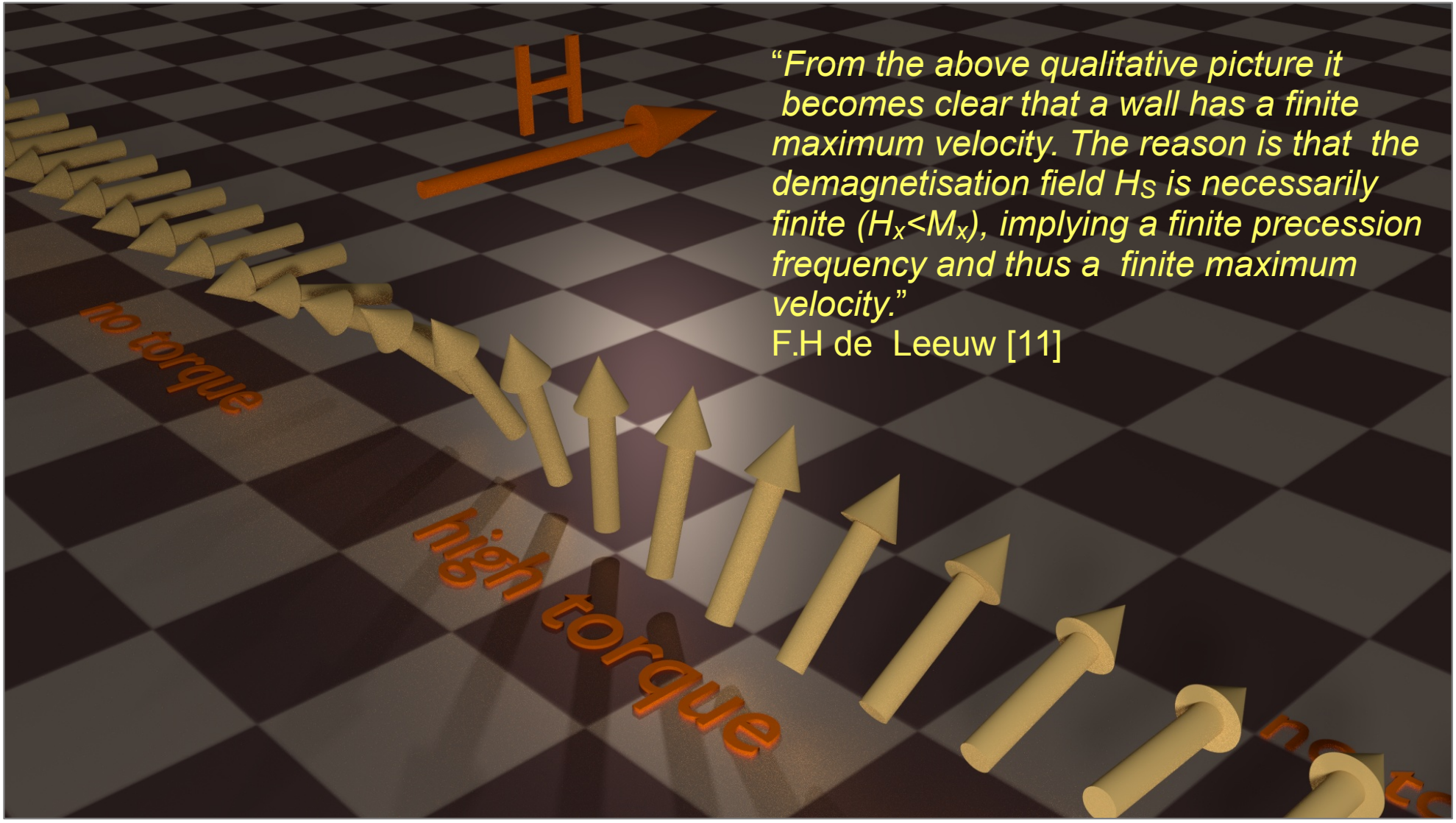

"From the above qualitative picture it becomes clear that a wall has a finite maximum velocity. The reason is that the demagnetisation field H_S is necessarily finite ($H_x<M_x$), implying a finite precession frequency and thus a finite maximum velocity."
F.H de Leeuw [11]

Domain wall mobility

- In relatively broad range of magnetic field the domain wall velocity is approximately linear function of the applied field [12].
- The velocity can be expressed as:

$$v(H)=\begin{cases} 0 & H < H_{dp} \\ \mu(|H|-H_{dp}) & H \geq H_{dp} \end{cases}$$

- Above depinning field H_{dp} the wall moves with velocity determined by mobility μ.
- Typical values of wall mobility are [12]:

- μ=1-1000 $ms^{-1}\ mT^{-1}$ ≈0.00125-1.25 $ms^{-1}\ (A/m)^{-1}$

- In thin films of permalloy the mobility is of the order of μ=100 $ms^{-1}\ mT^{-1}$[12].

$H < H_{dp}$

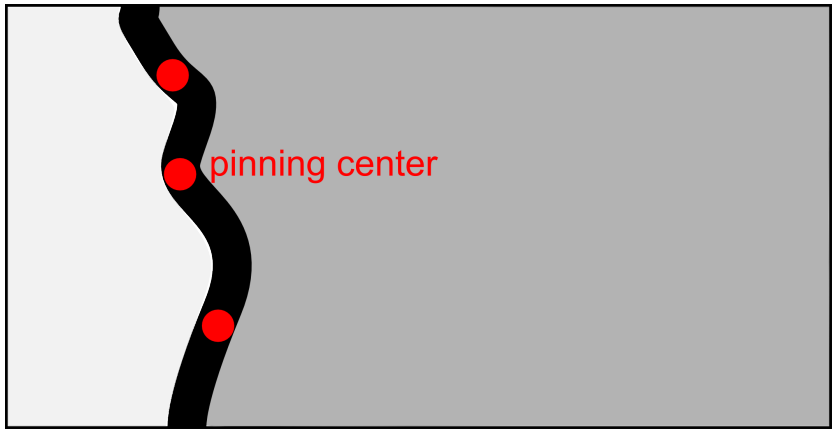

$H_{dp} \leq H$

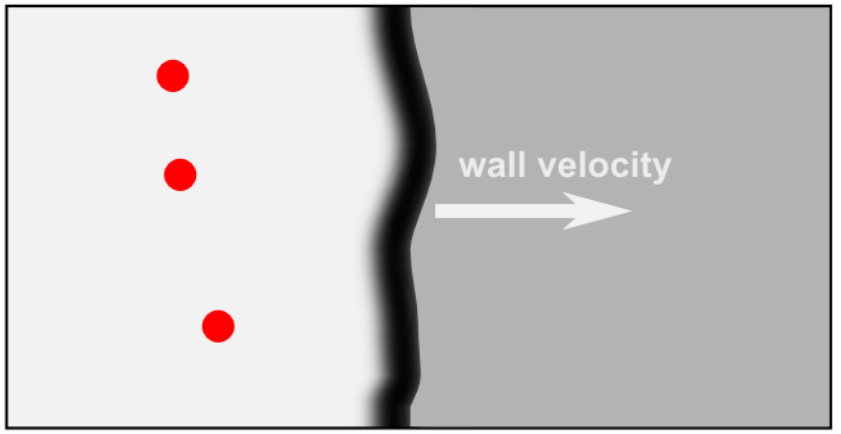

Domain wall mobility

- In relatively broad range of magnetic field the domain wall velocity is approximately linear function of the applied field [12].
- The velocity can be expressed as:

$$v(H)=\begin{cases} 0 & H < H_{dp} \\ \mu(|H|-H_{dp}) & H \geq H_{dp} \end{cases}$$

- Typical values of wall mobility are [12]:
- μ=1-1000 ms^{-1} mT^{-1}
- Velocity of domain walls in typical fields used in experiments can exceed **10 km/s**

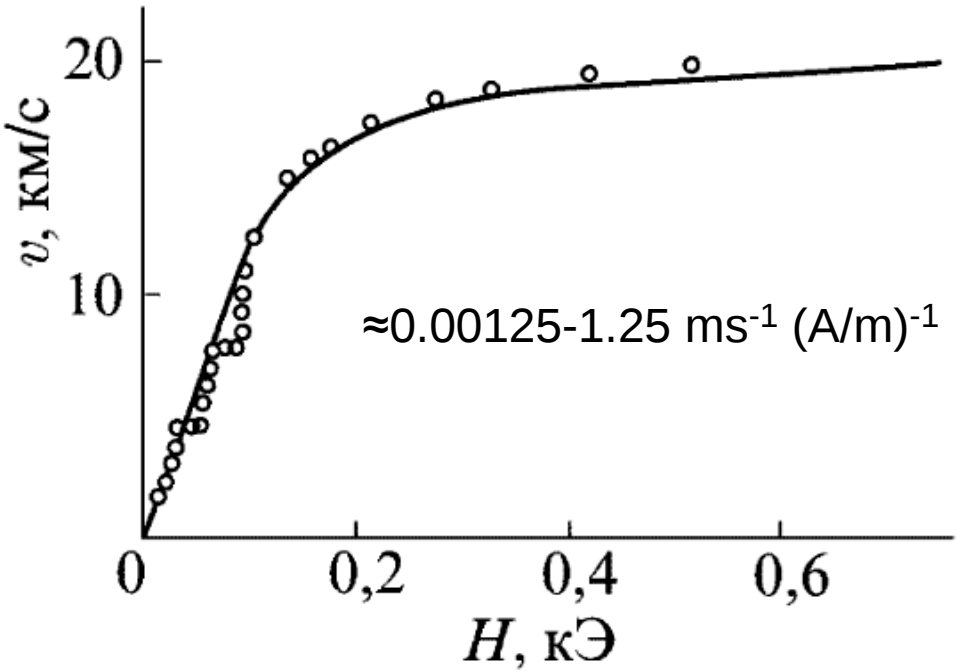

Рис. 26.3. Зависимость $v(H)$ для слабого ферромагнетика; точками показаны экспериментальные данные для иттриевого ортоферрита ($YFeO_3$)

image from: Боровик Е. С, Еременко В. В., Мильнер А. С. Лекции по магнетизму. , М.: ФИЗМАТЛИТ, 2005.

Domain wall in external magnetic field – thermally activated motion

- **Magnetic viscosity** - the delayed response of magnetic domains to changes in external field [13].
- The effect, called also *magnetic aftereffect*, is easily observable in ultrathin magnetic films.
- Cu(100)/Fe(7 ML) grown at RT
- Domain images were taken in-situ with the help of a *long-distance microscope* (the distance between the front of the microscope and the sample was 32 cm, the resolution was better than 10μm)

Relatively small (~10%) changes of the external field strength accelerate switching tenfold

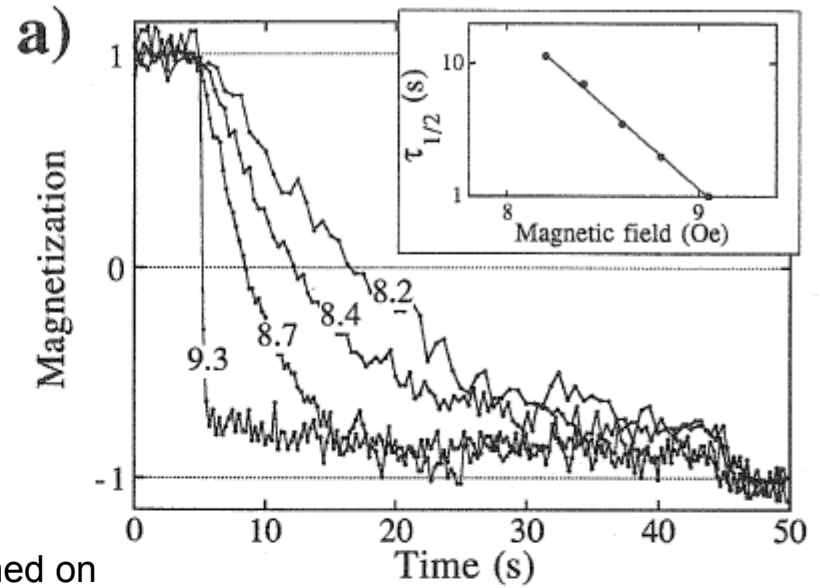

20s after field is switched on

5s after field is switched on

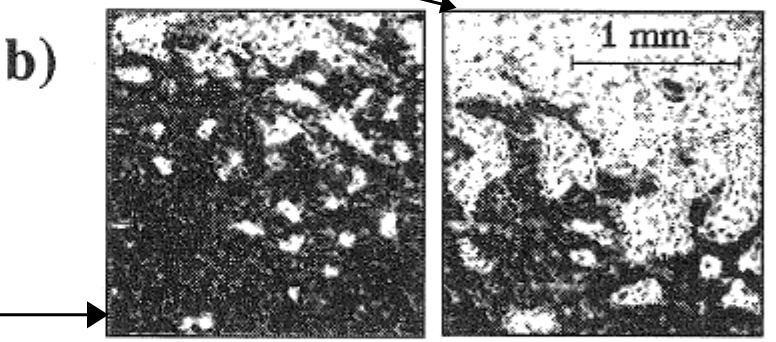

Fig. 5. (a) Magnetization relaxation curves for the sample III at different field values (indicated in the figure in Oe). (b) Domain images of the same location on the sample measured at constant magnetic field (8.2 Oe), but applied over different time (left panel – 5 s, right panel – 20 s).

A. Kirilyuk, J. Giergiel, J. Shen, J. Kirschner, Journal of Magnetism and Magnetic Materials **159**, L27 (1996)

Domain wall in external magnetic field – thermally activated motion

- Consider a domain wall crossing a sequence of potential barriers of equal* height E_0 [13].
- The energy that must be supplied to wall in the presence of field H in the direction of expanding domain is:

$$E = E_0 - \alpha H$$

, where αH is the energy supplied by the field during penetration of or the "climbing up" the barrier

- Number of occasions per second on which the wall acquires thermal energy E high enough to cross the barrier is:

$$N = C e^{-(E_0 - \alpha H)/kT}$$

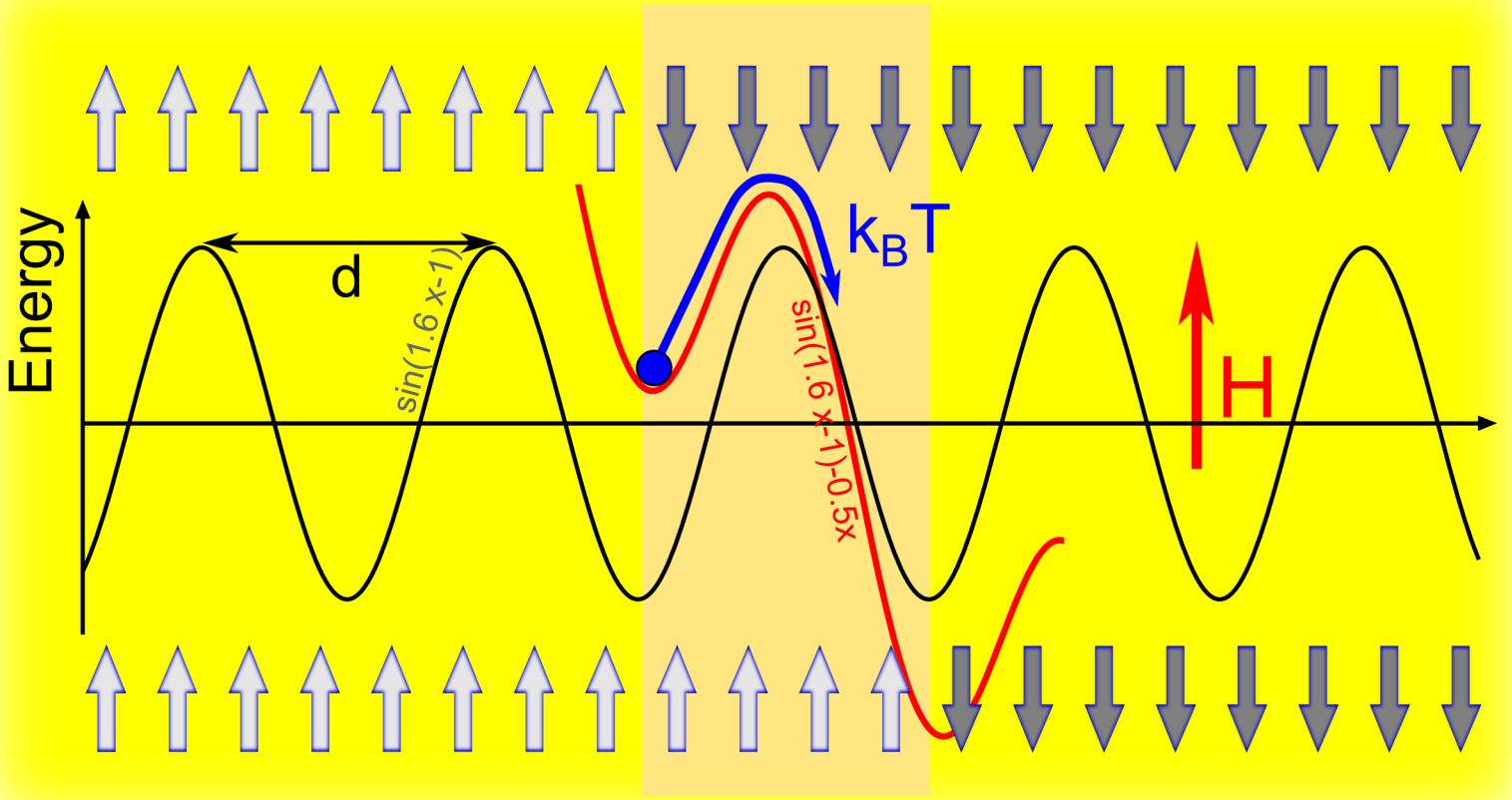

*for simplicity

Domain wall in external magnetic field – thermally activated motion

- Consider a domain wall crossing a sequence of potential barriers of equal* height E_0 [13].
- The energy that must be supplied to wall in the presence of field H in the direction of expanding domain is:

$$E = E_0 - \alpha H$$

, where αH is the energy supplied by the field during penetration of or the "climbing up" the barrier

- Number of occasions per second on which the wall acquires thermal energy E high enough to cross the barrier is:

$$N = C e^{-(E_0 - \alpha H)/kT}$$

, where C* is a constant of the order 10^9 to 10^{10} Hz [13,14,15]

- If the average separation of energy minima is d and the delay of the wall at each energy barrier is much greater than time to move from barrier to barrier then the wall velocity is**:

$$v = N d = d C e^{-(E_0 - \alpha H)/kT} \propto e^{H/kT}$$

$$v \propto e^{H/kT}$$

- In many cases the reversal takes place in limited volume V_B (Barkhausen or activation volume [16]) and the energy associated with the reversal can be expressed as:

$$\alpha H \rightarrow 2 \mu_0 M V_B H$$

, which comes from the Zeeman energy of reversing volume (fragment of the wall etc.)

*called attempt frequency [5]

**note that, in this formulation, th velocity is different from zero in the absence of field → ,,Brownian motion"

Sweep rate dependence of coercivity

- Dependence of coercivity on magnetic field sweep rate is common to superparamagnetic particles [15].
- In particulate magnetic media the deciding factor in defining magnetic properties is not the volume of a single particle but the so called switching (activation) volume [15].
- If theses volumes are close to each other it means that the particles switch almost independently.

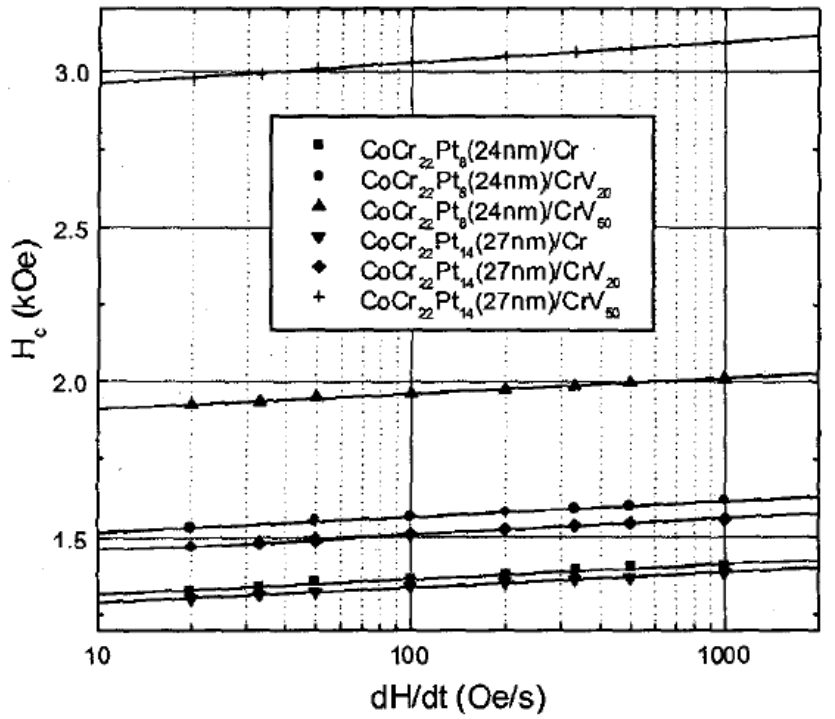

Fig. 1. Field sweep-rate (dH/dt) dependence of coercivity (H_c) of $CoCr_{22}Pt_8$(24nm)/CrV_x and $CoCr_{22}Pt_{14}$(27nm)/CrV_x films.

Mingjun Yu, M. F. Doerner, D. J. Sellmyer, IEEE Trans. Magn. **34**, 1534 (1998)

Eddy-current damping

- Eddy-currents (EC) - electric currents induced in a electrical *conductor* exposed to changing magnetic field.
- In magnetic materials the domain walls movement may produce changing field which create eddy currents.
- Eddy-currents are governed by Faraday's law
- In magnetic specimens the EC damping is more pronounced in the middle of the crystal which may lead, depending on the field value, to curving of the domain.
- **In bulk materials the field penetrates the inner regions of the sample with a delay** [18].
- The time required for the EC effect to disappear depends on resistivity and permeability of the material and the shape of the specimen.
- If the field applied to the rod is alternating then the maximum induction at the center of the specimen can be always less than the maximum field at its surface.

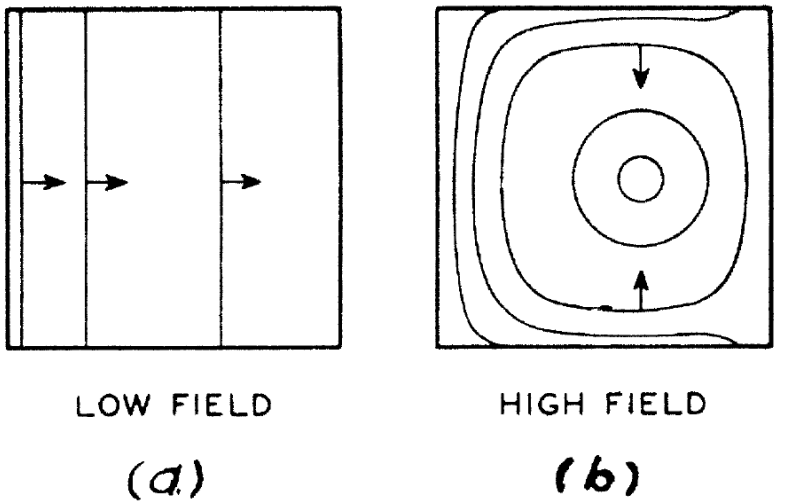

FIG. 2. Boundary motion in low and high fields.

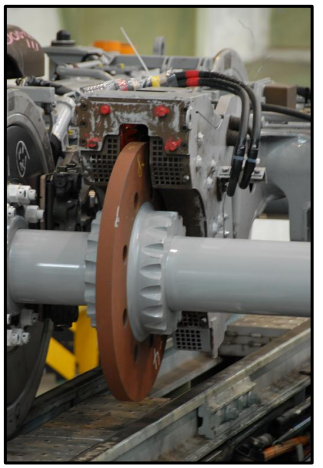

Eddy current brake equipment on Shinkansen series 700

from Wikimedia Commons; author: Take-y at ja.wikipedia

H. J. Williams, W. Shockley, and C. Kittel, Phys. Rev. 80, 1090 (1950)

Eddy-current damping

- Domain wall movement creates the eddy-currents which in turn (Lenz's rule) create the field opposing the applied field.
- The wall moves now in a effective field which is less than the applied field – the wall velocity diminishes.
- For the special case of the straight wall moving in a rod of square cross section expression for the velocity is [18]:

$$v(H) \approx 8 \times 10^{8} \frac{\pi \rho}{M_s d},$$

d -edge length

- Note is that the low resistivity materials are characterized high eddy-current damping and consequently low wall mobilities.
- Eddy-current damping depends on the geometry of the specimen

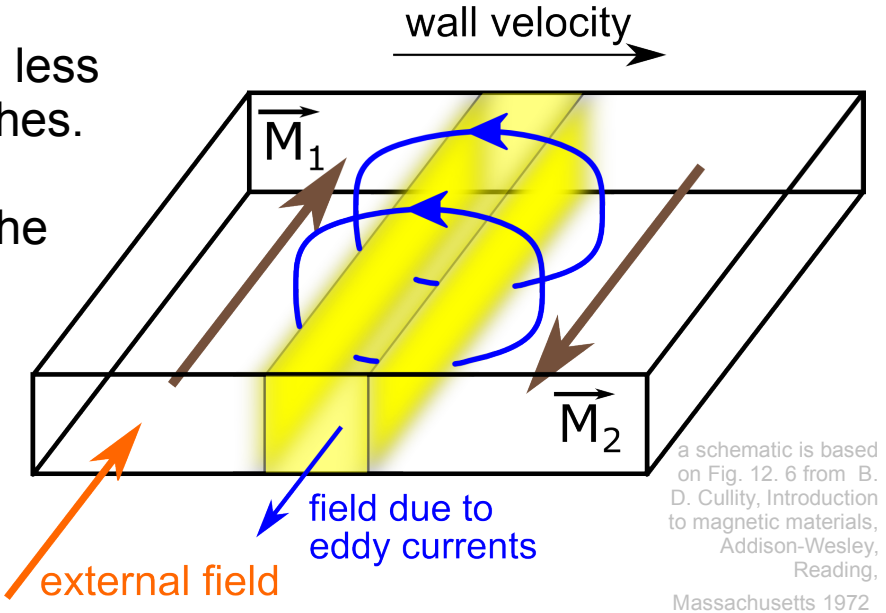

a schematic is based on Fig. 12. 6 from B. D. Cullity, Introduction to magnetic materials, Addison-Wesley, Reading, Massachusetts 1972

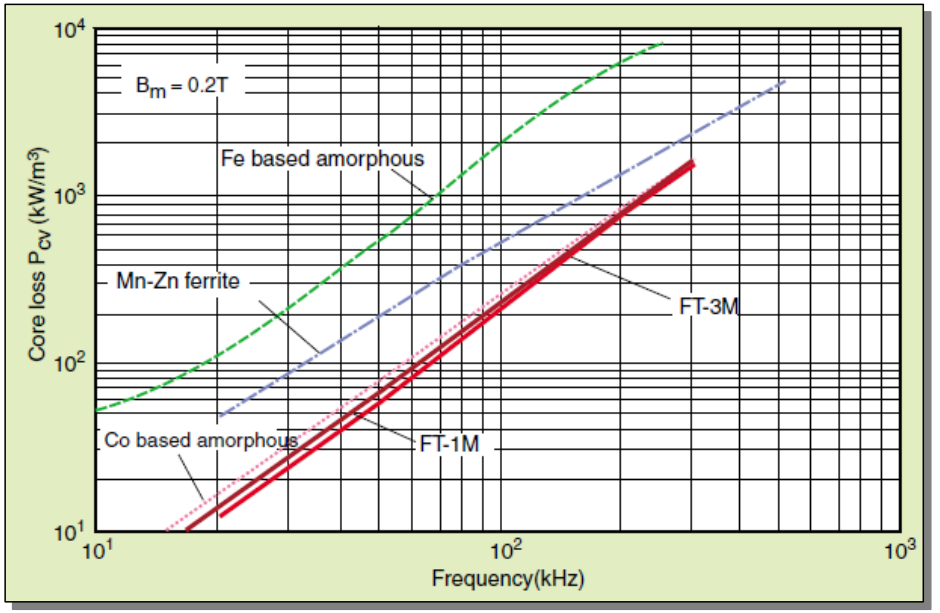

exemplary values of core losses in modern FINEMET® soft magnetic materials

image source HITACHI, www.hilltech.com/pdf/hl-fm10-cFinemetIntro.pdf.pdf

References

1. A. Hubert, R. Schäfer, Magnetic domains: the analysis of magnetic microstructures, Springer 1998
2. P. Суху, Магнитные Тонкие Пленки, Издательство МИР Москва 1967
3. W. Ketterle, MIT Physics 8.421 Atomic and optical Physics,
4. M. Getzlaff, Fundamentals of Magnetism, Springer-Verlag Berlin-Heidelberg 2008
5. H. Kronümller, General Micromagnetic Theory, in Handbook of Magnetism and Advanced Magnetic Materials, edited by H. Kronümller and S.S.P. Parkin, vol. 2, Wiley, 2007.
6. T. Gilbert, IEEE Trans. Magn. **40**, 3443 (2004)
7. J. Miltat and M. Donahue, Numerical micromagnetics: finite difference methods, in Handbook of Magnetism and Advanced Magnetic Materials, edited by H. Kronümller and S.S.P. Parkin, vol. 2, Wiley, 2007.
8. H. Kronmüller, M. Fähnle, Micromagnetism and the Microstructure of Ferromagnetic Solids, Cambridge University Press, 2003
9. A. Aharoni, Introduction to the Theory of Ferromagnetism, Clarendon Press, Oxford 1996
10. B. N. Filippov, M. N. Dubovik, and L. G. Korzunin, The Physics of Metals and Metallography **112**, 330 (2011)
11. F.H de Leeuw, R van den Doel and U. Enz, Rep. Prog. Phys. **43**, 689 (1980)
12. J.M.D. Coey, Magnetism and Magnetic Materials, Cambridge University Press 2009
13. F. D. Stacey, Aust. J. Phys. **13** , 599 (1960)
14. D. Siemers and E. Nembach, J. Appl. Phys. **5**, 4895 (1979)
15. Mingjun Yu, M. F. Doerner, D. J. Sellmyer, IEEE Trans. Magn. **34**, 1534 (1998)
16. M. Labrune, S. Andrieu, F. Rio, P. Bernstein, JMMM **80**, 211 (1989)
17. I. Ruiz-Feal, T. A. Moore, L. Lopez-Diaz, and J. A. C. Bland, Phys. Rev. B **65**, 054409 (2002)
18. B. D. Cullity, Introduction to magnetic materials, Addison-Wesley, Reading, Massachusetts 1972